Journal of Computational Mathematics
Vol.xx, No.x, 2026, 1–25.

http://www.global-sci.org/jcm
doi:10.4208/jcm.2509-m2024-0222

A MULTIPLE-INVARIANTS PRESERVING SCHEME FOR MODIFIED TWO-COMPONENT EULER-POINCARÉ EQUATIONS*

Boya Zhou
School of Mathematics, Foshan University, Foshan 52800, China
Email: byzhou@fosu.edu.cn
Ruimin Gao[1)]
School of Mathematics and Statistics, Huazhong University of Science and Technology, Wuhan 430074, China
Email: ruimingao@hust.edu.cn
Qifeng Zhang
Department of Mathematics, Zhejiang Sci-Tech University, Hangzhou 310018, China
Email: zhangqifeng0504@gmail.com

Abstract

This paper presents a high-order multiple-invariants preserving numerical scheme for the modified Euler-Poincaré equations with two components. It is shown that the scheme preserves at least three invariants: mass, momentum and energy. In contrast, the previous schemes usually keep only one or two. Meanwhile, the scheme achieves high order accuracy in spatial direction as well as second-order in time, which will be proved rigorously in this paper. The key to the present scheme aims at the construction of a bi-variate function and utilization of a special time discretization. Numerical tests are given to verify the theoretical findings.

Mathematics subject classification: 65M06, 65M12, 35Q53.
Key words: Modified two-component Euler-Poincaré equations, Bi-variate function, Mass conservation, Preserving energy, Momentum conservation.

1. Introduction

Shallow water waves equations (SWWEs) are usually used to describe the dynamics of shallow water waves created by the freesurface of light water body, where the depth of the water is much smaller than the wavelength. Since this shallow water model was introduced, it has been gained significant importance and owned wide application in serval areas, tsunami, atmospheric circulation, open channels and rivers, among others [3, 24, 37, 53, 54]. SWWEs in geophysical fluid dynamics (GFD) attract many researchers' eyes based on containing some of the vital dynamical features in terms of atmosphere and ocean. Pedlosky [35] presented the shallow water model with some assumptions. Tan [39] pointed out that two-dimension shallow water was regarded as a compressible plane flow introduced by a virtual gas in a special way. Caviedes-Voullième *et al.* [6] studied SWWEs in order to simulate rainfall-runoff processes. He compared the performance of zero-inertia (diffusive wave) with shallow water model and found

* Received October 10, 2024 / Revised version received June 23, 2025 / Accepted September 8, 2025 / Published online February 27, 2026 /
1) Corresponding author

that this solver paid less computational time. More studies about SWWEs in GFD can be found in [14, 16, 38, 48].

As pointed in [19, 20], one can invert some standard GFD into Euler-Poincaŕe form with putting serval suitable assumptions and the properties of Lagrangian. The Euler-Poincaré equation is widely used for modeling and studying phenomena across various fluid dynamics subfields. Such equation combines the integrability property, and compressibility with the free-surface elevation dynamics which appears in the region of shallow water [21]. Since such equation contains many higher order derivatives and complex nonlinear terms, the corresponding theoretical analysis and efficient numerical scheme constructions are difficult to achieve.

In this paper, we construct a method which is structure-preserving to solve the following modified two-component Euler-Poincaré equation (MEP2):

$$\begin{cases} m_t + um_x + 2mu_x + g\rho\bar{\rho}_x = 0, & t > 0, \quad x \in \mathbb{R}, \\ \rho_t + (\rho u)_x = 0, & t > 0, \quad x \in \mathbb{R}, \\ m = \big(\mathcal{I} - \alpha\partial_x^2\big)u, \quad \rho = \big(\mathcal{I} - \beta\partial_x^2\big)(\bar{\rho} - \rho_0), & t > 0, \quad x \in \mathbb{R} \end{cases} \tag{1.1}$$

with the periodic boundary conditions

$$\rho(t, x + L) = \rho(t, x), \quad u(t, x + L) = u(x, t), \quad t > 0, \quad x \in \mathbb{R},$$

and the initial conditions

$$\bar{\rho}(0, x) = \bar{\rho}_0(x), \quad u(0, x) = u_0(x), \quad x \in \mathbb{R},$$

where m is the momentum, ρ is the density, u is the horizontal fluid velocity, $\bar{\rho}$ is locally average density, $\bar{\rho}_0$ is a constant, $\alpha, \beta > 0$ are dispersion parameters and g is a positive constant which means an acceleration caused by gravity. It is worth to point out that (1.1) has three invariants in theory [44],

$$\begin{aligned} &\text{Energy:} && \frac{\mathrm{d}}{\mathrm{d}t}\int_{\mathbb{R}} \left(g|\gamma|^2 + g\beta|\nabla\gamma|^2 + |u|^2 + \alpha|\nabla u|^2\right)(t, x)\mathrm{d}x = 0, \quad \gamma = \bar{\rho} - \rho_0, \\ &\text{Mass:} && \frac{\mathrm{d}}{\mathrm{d}t}\int_{\mathbb{R}} \rho(t, x)\mathrm{d}x = 0, \\ &\text{Momentum:} && \frac{\mathrm{d}}{\mathrm{d}t}\int_{\mathbb{R}} m(t, x)\mathrm{d}x = 0. \end{aligned}$$

Numerous effort has been done to the study of some special Euler-Poincaré equations ($\rho \equiv 0$ in Eq. (1.1)),

$$m_t + um_x + 2mu_x = 0, \quad m = u - u_{xx}, \quad x \in \mathbb{R}, \quad t > 0, \tag{1.2}$$

which is employed in profiling the unidirectional propagation of shallow water waves over a flat bottom [4]. The global conservation solutions of (1.2) have been obtained by Bressan and Constantin [2] depending continuously on the initial data. Furthermore, many numerical schemes have been applied for solving Eq. (1.2) such as the Galerkin methods [31,43], the spectral methods [36, 42] and the finite difference schemes [9, 18] and the operator splitting methods [17]. In order to make the equation more general and consistent with the real ocean system, some studiers turn their points into an extended equation named a two-component integrable system (EP2) which contains velocity and density variables

$$\begin{cases} m_t + um_x + 2u_x m + g\rho\rho_x = 0, & t > 0, \quad x \in \mathbb{R}, \\ \rho_t + (u\rho)_x = 0, & t > 0, \quad x \in \mathbb{R}, \\ m = \big(1 - \alpha\delta_x^2\big)u, & t > 0, \quad x \in \mathbb{R}. \end{cases} \tag{1.3}$$

The specific scheme (1.3) and its theoretical analysis could be found in [7, 11, 12]. Its mathematical properties have been considered further in some works [29, 30, 52]. While, as pointed out at [10], (1.3) has the disadvantage that the singular solution does not appear in term of density variable. Holm *et al.* [21] produced the system MEP2 and proved that the equation possesses peak solutions in the velocity but also emerges the singular solutions in both variables. They gave numerical results for the modified system and compared with (1.3) to verify their theoretical conclusions. Later, the global solution and blow up phenomena of (1.1) in high dimensional cases were studied analytically in [44]. However, the numerical solutions of two-component Euler-Poincaré equation (EP2) are still in great demand.

Constructing the numerical schemes to preserve some original physical properties of the equation is of great importance in applications. Up to now, energy-conserving and/or mass-conserving numerical schemes of the special Euler-Poincaré have shown significant advantage in lone-time simulations, see e.g., [22,30,34,45,49,51]. In order to solve (1.2), Matsuo [32] and Matsuo and Yamaguchi [33] established a Hamilton-conserving and energy-conserving scheme, respectively, which were based on Galerkin methods. Wang [41] constructed an energy-preserving finite difference scheme for solving generalized Euler-Poincaré equation (1.2). They presented rigorous proof of the unique solvability, energy conservation, stability and the fourth order convergence in the spatial direction. To be mentioned that there are several approaches developed to preserve invariants, such as invariant energy quadratization [46, 47], the relaxation approach [23, 25–27], scalar auxiliary variable approach [1, 5] and so on [28, 40, 50]. These methods usually can preserve no more than two invariants. To be mentioned, Zhang *et al.* [52] proposed a second-order nonlinear implicit scheme to solve a modified Camassa-Holm system ($\alpha = 1, \beta = 0, g = 1$ in (1.1)), and they proved the scheme can preserve at least three discrete conservation invariants. The multiple-invariants preserving scheme of MEP2 (1.1) has not been covered.

Inspired by [13, 52], the main goal of this paper is to propose a high-order and structure-preserving difference scheme to solve MEP2 (1.1), which satisfies the momentum, mass, and energy conserved discretely. The numerical structure was cast as follows. The space discretization is done by a bi-variate function $\psi(u, v)$ with considering the nonlinear derivative is complex and high order, as well as the nonlinear terms are coupled. The time discretization is done by implicit Crank-Nicolson scheme. Then, we obtain a three-invariants-preserving scheme with reaching second order and fourth order accuracy in time and space, respectively. Such error estimate satisfies without any restriction on the value of parameters α, β.

The key to the structure-preserving scheme is the choice of a special time discretization and a bi-variate function $\psi(u, v)$. The bi-variate function is obtained by the idea of a linear combination of u and v and some high-order difference schemes. The skills to discrete space derivative also were used in our paper [13] to solve EP2, where we only proposed the scheme that kept two invariants. Thanks to the bi-variate function and the special time discretization, the structure-preserving scheme solving MEP2 is obtained. Moreover, the fully-discrete scheme whose spatial convergent result is fourth order is shown to be second-order convergent in time, which is proved rigorously with applying the discrete Grönwall inequality. We believe that this paper is the first to conduct a scheme to keep three invariants but also achieve fourth order convergence in space for MEP2 (1.1).

The rest of the paper is structured in the following way. In Section 2, we apply the second order finite different method for the temporal discretization and a modified bi-variate function is used for the space derivative. Moreover, we derive a three conservative invariants preserving

scheme and prove it. The convergence analysis of the previous scheme can be found in Section 3. Based on the properties of the bivariate function and the discrete Grönwall inequality, we provide the proof. Several numerical experiments are presented to verify our theoretical findings in Section 4. A conclusion is displayed in Section 5.

2. Numerical Scheme and Main Results

We will present a new finite difference scheme and give some numerical conserving results in this part.

2.1. Fully discrete numerical scheme

In order to introduce our scheme conveniently, some notations will be given. Let M, N be the positive integers, and set $\Delta t = T/N, \Delta h = L/M$. Define the grid points

$$\Omega_{h,\,t} = \{(x_i, t_k) \,|\, t_k = k\Delta t,\ 0 \le k \le N,\ x_i = i\Delta h,\ 0 \le i \le M\}$$

and an index set $P_M = \{i \,|\, 1 \le i \le M\}$. For any grid functions,

$$u = \{u_j^n \,|\, 1 \le j \le M,\ 0 \le n \le N\},$$
$$v = \{v_j^n \,|\, 1 \le j \le M,\ 0 \le n \le N\},$$

we define

$$\big(u_j^n\big)_{\bar{x}} = \frac{u_{j+1}^n - u_j^n}{\Delta h}, \qquad \big(u_j^n\big)_{\bar{\bar{x}}} = \frac{u_j^n - u_{j-1}^n}{\Delta h},$$
$$\big(u_j^n\big)_{\dot{x}} = \frac{u_{j+1}^n - u_{j-1}^n}{2\Delta h}, \quad \big(u_j^n\big)_{\ddot{x}} = \frac{u_{j+2}^n - u_{j-2}^n}{4\Delta h},$$
$$\delta_t u_j^{n+\frac{1}{2}} = \frac{u_j^{n+1} - u_j^n}{\Delta t}, \qquad u_j^{n+\frac{1}{2}} = \frac{1}{2}\big(u_j^n + u_j^{n+1}\big),$$
$$\varphi_1\big(u_j^n\big) = \frac{4}{3}\frac{u_{j+1}^n - u_{j-1}^n}{2\Delta h} - \frac{1}{3}\frac{u_{j+2}^n - u_{j-2}^n}{4\Delta h},$$
$$\varphi_2\big(u_j^n\big) = \frac{4}{3}\frac{u_{j+1}^n - 2u_j^n + u_{j-1}^n}{\Delta h^2} - \frac{1}{3}\frac{u_{j+2}^n - 2u_j^n + u_{j-2}^n}{4\Delta h^2},$$
$$\psi(u^n, v^n)_j = \frac{4}{3}\big[u_j^n\big(v_j^n\big)_{\dot{x}} + \big((u^n v^n)_j\big)_{\dot{x}}\big] - \frac{1}{3}\big[u_j^n\big(v_j^n\big)_{\ddot{x}} + \big((u^n v^n)_j\big)_{\ddot{x}}\big],$$
$$\psi\big(\varphi_2(u^n), v^n\big)_j = \frac{4}{3}\big[\varphi_2\big(u_j^n\big)\big(v_j^n\big)_{\dot{x}} + \big(\varphi_2\big(u_j^n\big)v_j^n\big)_{\dot{x}}\big] - \frac{1}{3}\big[\varphi_2\big(u_j^n\big)\big(v_j^n\big)_{\ddot{x}} + \big(\varphi_2\big(u_j^n\big)v_j^n\big)_{\ddot{x}}\big],$$

where $(u^n v^n)_j$ represents $u_j^n v_j^n$. Furthermore, we define

$$U_h = \{v \,|\, v = (v_i),\ v_{i+M} = v_i,\ i \in \mathbb{Z}\}.$$

Then, for any grid function $u, v \in U_h$, we define a discrete inner product and its norms as

$$(u, v) = \Delta h \sum_{i \in P_M} u_i v_i, \quad \|u\| = \sqrt{(u, u)}, \quad \|u\|_1 = \sqrt{-\big(\varphi_2(u), u\big)}, \tag{2.1}$$

$$\|u_{\dot{x}}\| = \sqrt{\Delta h \sum_{i \in P_M} |(u_i)_{\dot{x}}|^2}, \quad \|u_{\ddot{x}}\| = \sqrt{\Delta h \sum_{i \in P_M} |(u_i)_{\ddot{x}}|^2}. \tag{2.2}$$

Based on this foundation, we introduce fourth-order formulas for the first and second derivative, respectively, as presented in [40].

Lemma 2.1 ([40]) *For any smooth functions u, v, suppose $U_i^k = u(x_i, t_k),\ i \in P_M, t_k = k\Delta t$, we have*

$$\frac{4}{3}\frac{U_{i+1}^k - U_{i-1}^k}{2\Delta h} - \frac{1}{3}\frac{U_{i+2}^k - U_{i-2}^k}{4\Delta h} = \frac{dU_i^k}{dx} + \mathcal{O}(\Delta h^4),$$
$$\frac{4}{3}\frac{U_{i+1}^k - 2U_i^k + U_{i-1}^k}{\Delta h^2} - \frac{1}{3}\frac{U_{i+2}^k - 2U_i^k + U_{i-2}^k}{4\Delta h^2} = \frac{d^2U_i^k}{dx^2} + \mathcal{O}(\Delta h^4).$$

Together with Lemma 2.1 and Taylor's expansion, the following result can be obtained, which is the key point for estimating the bi-variate function. As it has been proved in our another paper [13], we only display it here.

Lemma 2.2 ([13]) *For any smooth functions u, v, suppose $U_i^k = u(x_i, t_k), i \in P_M, t_k = k\Delta t$. Then, we have*

$$\psi(U^n, U^n)_i = 3U_i^k \frac{dU_i^k}{dx} + \mathcal{O}(\Delta h^4),$$
$$\psi\big(\varphi_2(U^n), U^n\big)_i = U_i^k \frac{d^3U_i^k}{dx^3} + 2\frac{dU_i^k}{dx}\frac{d^2U_i^k}{dx^2} + \mathcal{O}(\Delta h^4).$$

Now, we start to establish a fully implicit finite difference scheme with using the Crank-Nicolson scheme in time discretization. For this purpose, we let $U_j^n = u(x_j, t_n),\ \bar{\Phi}_j^n = \bar{\rho}(x_j, t_n)$ and $\Phi_j^n = \rho(x_j, t_n)$. Considering (1.1) at the point $(x_j, t_{n+1/2}), j \in P_M, 0 \le n \le N$, we have

$$\delta_t U_j^{n+\frac{1}{2}} - \alpha\delta_t\varphi_2\big(U_j^{n+\frac{1}{2}}\big) + \psi\big(U^{n+\frac{1}{2}}, U^{n+\frac{1}{2}}\big)_j + \alpha\psi\big(\varphi_2\big(U^{n+\frac{1}{2}}\big), U^{n+\frac{1}{2}}\big)_j + g\Phi_j^{n+\frac{1}{2}}\varphi_1\big(\bar{\Phi}_j^{n+\frac{1}{2}}\big) = R_j^n, \tag{2.3}$$
$$\delta_t\bar{\Phi}_j^{n+\frac{1}{2}} - \beta\delta_t\varphi_2\big(\bar{\Phi}_j^{n+\frac{1}{2}}\big) + \varphi_1\big(\Phi^{n+\frac{1}{2}}U^{n+\frac{1}{2}}\big)_j = Q_j^n, \tag{2.4}$$
$$U_j^n = U_{j+M}^n, \quad \Phi_j^n = \Phi_{j+M}^n, \tag{2.5}$$

where R^n and Q^n are the local truncation errors, which can be estimated from Lemmas 2.1 and 2.2,

$$|R^n| \le c_1(\Delta t^2 + \Delta h^4), \quad |Q^n| \le c_1(\Delta t^2 + \Delta h^4), \quad j \in P_M$$

with c_1 being a positive constant independent of Δt and Δh.

Replacing the exact solutions U_j^n with the numerical approximation u_j^n, and ignoring the truncation error, the finite different scheme for any $j \in P_M, 0 \le n \le N$ reads

$$\delta_t u_j^{n+\frac{1}{2}} - \alpha\delta_t\varphi_2\big(u_j^{n+\frac{1}{2}}\big) + \psi\big(u^{n+\frac{1}{2}}, u^{n+\frac{1}{2}}\big)_j - \alpha\psi\big(\varphi_2(u^{n+\frac{1}{2}}), u^{n+\frac{1}{2}}\big) + g\rho_j^{n+\frac{1}{2}}\varphi_1\big(\bar{\rho}_j^{n+\frac{1}{2}}\big) = 0, \tag{2.6}$$
$$\delta_t\bar{\rho}_j^{n+\frac{1}{2}} - \beta\delta_t\varphi_2\big(\bar{\rho}_j^{n+\frac{1}{2}}\big) + \varphi_1\big(\rho_j^{n+\frac{1}{2}}u_j^{n+\frac{1}{2}}\big) = 0, \tag{2.7}$$
$$u_j^n = u_{j+M}^n, \quad \rho_j^n = \rho_{j+M}^n. \tag{2.8}$$

The main properties of the fully discrete scheme will be proposed in the following subsection. The implement of our numerical schemes with detailed algorithm flow chart is shown in the Appendix A.

2.2. Structure-preserving results

In this section, we will present the structure-preserving conclusions and their detailed proof. Before we prove our main results, some lemmas are given.

Lemma 2.3 ([15]) *For any grid functions $u, v \in U_h$, we have*

$$\begin{aligned}
&(u_{\bar{\bar{x}}}, v) = -(u, v_{\bar{\bar{x}}}), && (u_{\bar{x}}, v) = -(u, v_{\bar{x}}), && (u_{\ddot{x}}, v) = -(u, v_{\ddot{x}}),\\
&\big(\varphi_1(u), v\big) = -\big(u, \varphi_1(v)\big), && (u_{\ddot{x}}, u) = 0, && (u_{\hat{x}}, u) = 0.
\end{aligned}$$

Lemma 2.4 ([13]) *For any grid functions $u, v \in U_h$, we have*

$$(\psi(u, v), v) = 0, \quad \big(\psi(\varphi_2(u), v\big), v) = 0, \tag{2.9}$$

$$\|u_{\ddot{x}}\| \le \|u_{\dot{x}}\| \le \|u\|_1. \tag{2.10}$$

Lemma 2.5. *For any grid functions $u, v \in U_h$, we have*

$$\big(\psi(u, v), 1\big) = 0, \tag{2.11}$$

$$\big(\psi\big(\varphi_2(u), v\big), 1\big) = 0, \tag{2.12}$$

$$\big(\varphi_1(u), v\big) = 0, \quad v = u - \varepsilon\varphi_2(u), \quad \varepsilon > 0. \tag{2.13}$$

Proof. By Lemmas 2.3 and 2.4, we have

$$\begin{aligned}
\big(\psi(u, v), 1\big) &= \frac{4}{3}\sum_{j\in P_M}\big[u_j(v_{\dot{x}})_j + \big((uv)_j\big)_{\dot{x}}\big] - \frac{1}{3}\sum_{j\in P_M}\big[u_j(v_{\ddot{x}})_j + \big((uv)_j\big)_{\ddot{x}}\big]\\
&= \frac{4\Delta h}{3}\sum_{j\in P_M} u_j\frac{v_{j+1}-v_{j-1}}{2\Delta h} - \frac{\Delta h}{3}\sum_{j\in P_M} u_j\frac{v_{j+2}-v_{j-2}}{4\Delta h}\\
&= \frac{2}{3}\sum_{j\in P_M}\big[u_j\big(u_{j+1}-\varepsilon\varphi_2(u_{j+1})\big) - u_j\big(u_{j-1}-\varepsilon\varphi_2(u_{j-1})\big)\big]\\
&\quad + \frac{1}{12}\sum_{j\in P_M}\big[u_j\big(u_{j+2}-\varepsilon\varphi_2(u_{j+2})\big) - u_j\big(u_{j-2}-\varepsilon\varphi_2(u_{j-2})\big)\big]\\
&= -\frac{2\varepsilon}{3\Delta h^2}\sum_{j\in P_M}[u_j(u_{j+2}-2u_{j+1}+u_j) - u_j(u_j-2u_{j-1}+u_{j-2})]\\
&\quad - \frac{\varepsilon}{48\Delta h^2}\sum_{j\in P_M}[u_j(u_{j+3}-4u_{j+1}+u_{j-1}) - u_j(u_{j+1}-4u_{j-1}+u_{j-3})]\\
&= -\frac{2\varepsilon}{3\Delta h^2}\sum_{j\in P_M}[(u_ju_{j+2}-u_ju_{j-2}) - 2(u_ju_{j+1}-u_ju_{j-1})]\\
&\quad - \frac{\varepsilon}{48\Delta h^2}\sum_{j\in P_M}[(u_ju_{j+3}-u_ju_{j-3}) - 4(u_ju_{j+1}-u_ju_{j-1})\\
&\qquad + (u_ju_{j-1}-u_ju_{j+1})] = 0.
\end{aligned}$$

Since

$$\begin{aligned}
\big(\varphi_1(u), v\big) &= \frac{4\Delta h}{3}\sum_{j\in P_M}(u_{\dot{x}}, v) - \frac{\Delta h}{3}\sum_{j\in P_M}(u_{\ddot{x}}, v)\\
&= -\left[\frac{4\Delta h}{3}\sum_{j\in P_M}(u, v_{\dot{x}}) - \frac{\Delta h}{3}\sum_{j\in P_M}(u, v_{\ddot{x}})\right]
\end{aligned}$$

$$= \frac{4\Delta h}{3}\sum_{j\in P_M} u_j\frac{v_{j+1}-v_{j-1}}{2\Delta h} - \frac{\Delta h}{3}\sum_{j\in P_M} u_j\frac{v_{j+2}-v_{j-2}}{4\Delta h},$$

we can prove (2.12) and (2.13) in a similar way as (2.11). □

Let $\gamma_j^n = \bar{\rho}_j^n - \rho_0$, we present the discrete counterparts of energy, mass and momentum

$$\begin{aligned}
&\text{Energy:} && E^n = \|u^n\|^2 + \alpha\|u^n\|_1^2 + g\big(\|\gamma^n\|^2 + \beta\|\gamma^n\|_1^2\big), && 0\le n\le N,\\
&\text{Mass:} && I_1^n = \Delta h\sum_{j\in P_M}\rho_j^n = (\rho^n,\mathbf{1}), && 0\le n\le N,\\
&\text{Momentum:} && I_2^n = \Delta h\sum_{j\in P_M} m_j^n = (m^n,\mathbf{1}), && 0\le n\le N,
\end{aligned}$$

where

$$m_j^n = u_j^n - \alpha\varphi_2\big(u_j^n\big). \tag{2.14}$$

Next, the theoretical results of conservations are given.

Theorem 2.1. *Let* $\{u_j^n,\rho_j^n,\bar{\rho}_j^n \,|\, j\in P_M, 0\le n\le N\}$ *be the solution of* (2.6)-(2.8). $\{m_j^n \,|\, j\in P_M, 0\le n\le N\}$ *is defined in* (2.14). *For any* $1\le n\le N$, *we have*

$$E^n = E^0,\quad I_1^n = I_1^0,\quad I_2^n = I_2^0.$$

Proof. Since $\bar{\rho}_0$ is a constant, for any $j\in P_M, 0\le n\le N$, (2.6)-(2.7) is equivalent to

$$\begin{aligned}
&\delta_t u_j^{n+\frac12} - \alpha\delta_t\varphi_2 u_j^{n+\frac12} + \psi\big(u^{n+\frac12},u^{n+\frac12}\big)_j\\
&\quad - \alpha\psi\big(\varphi_2\big(u^{n+\frac12}\big),u^{n+\frac12}\big)_j + g\rho_j^{n+\frac12}\varphi_1\big(\gamma_j^{n+\frac12}\big) = 0,
\end{aligned}\tag{2.15}$$

$$\delta_t\gamma_j^{n+\frac12} - \beta\delta_t\varphi_2\big(\gamma_j^{n+\frac12}\big) + \varphi_1\big(\rho_j^{n+\frac12}u_j^{n+\frac12}\big) = 0,\quad j\in P_M. \tag{2.16}$$

Step 1. We prove the conservation of energy. Taking the inner product of (2.15) with $u^{n+1/2}$ and applying Lemma 2.3, we get

$$\frac{1}{2\Delta t}\big(\|u^{n+1}\|^2 - \|u^n\|^2\big) + \frac{\alpha}{2\Delta t}\big(\|u^{n+1}\|_1^2 - \|u^n\|_1^2\big) = g\big(\gamma^{n+\frac12},\varphi_1\big(\rho^{n+\frac12}u^{n+\frac12}\big)\big). \tag{2.17}$$

Next, taking the inner product of (2.16) with $\gamma^{n+1/2}$ and using (2.1), we have

$$\frac{1}{2\Delta t}\big(\|\gamma^{n+1}\|^2 - \|\gamma^n\|^2\big) + \frac{\beta}{2\Delta t}\big(\|\gamma^{n+1}\|_1^2 - \|\gamma^n\|_1^2\big) + \big(\varphi_1\big(\rho^{n+\frac12}u^{n+\frac12}\big),\gamma^{n+\frac12}\big) = 0. \tag{2.18}$$

Multiplying (2.18) with g, and summing up with (2.17), we get

$$\begin{aligned}
&\frac{1}{2\Delta t}\big[\big(\|u^{n+1}\|^2 - \|u^n\|^2\big) + \alpha\big(\|u^{n+1}\|_1^2 - \|u^n\|_1^2\big)\big]\\
&\quad + \frac{g}{2\Delta t}\big[\big(\|\gamma^{n+1}\|^2 - \|\gamma^n\|^2\big) + \beta\big(\|\gamma^{n+1}\|_1^2 - \|\gamma^n\|_1^2\big)\big] = 0.
\end{aligned}\tag{2.19}$$

Rearranging (2.19), we can obtain

$$\begin{aligned}
&\|u^{n+1}\|^2 + \alpha\|u^{n+1}\|_1^2 + g\|\gamma^{n+1}\|^2 + g\beta\|\gamma^{n+1}\|_1^2\\
&= \|u^n\|^2 + \alpha\|u^n\|_1^2 + g\|\gamma^n\|^2 + g\beta\|\gamma^n\|_1^2,
\end{aligned}$$

which implies

$$E^{n+1} = E^n. \tag{2.20}$$

Step 2. We prove the conservation of mass. Taking the inner product of (2.16) with $\mathbf{1} := (1, 1, \ldots, 1)^\top \in U_h$, we have

$$\big(\delta_t \bar{\rho}^{n+\frac{1}{2}}, \mathbf{1}\big) - \beta\big(\delta_t \varphi_2\big(\bar{\rho}^{n+\frac{1}{2}}\big), \mathbf{1}\big) + \big(\varphi_1\big(\rho^{n+\frac{1}{2}} u^{n+\frac{1}{2}}\big), \mathbf{1}\big) = 0. \tag{2.21}$$

Applying Lemma 2.3, (2.21) can be rewritten as

$$(\rho^{n+1}, \mathbf{1}) = (\rho^n, \mathbf{1}),$$

which implies

$$I_1^{n+1} = I_1^n. \tag{2.22}$$

Step 3. We prove the conservation of momentum. Taking the inner product of (2.15) with $\mathbf{1} \in U_h$ and using Lemma 2.5, we have

$$\begin{aligned} &\big(\delta_t m^{n+\frac{1}{2}}, \mathbf{1}\big) + \big(\psi\big(m^{n+\frac{1}{2}}, u^{n+\frac{1}{2}}\big), \mathbf{1}\big) + g\big(\rho^{n+\frac{1}{2}} \varphi_1\big(\gamma^{n+\frac{1}{2}}\big), \mathbf{1}\big) \\ &= \big(\delta_t m^{n+\frac{1}{2}}, \mathbf{1}\big) = \frac{1}{\Delta t}(m^{n+1} - m^n) = 0, \end{aligned}$$

which implies

$$I_2^{n+1} = I_2^n. \tag{2.23}$$

Thus, it completes the proof. □

Corollary 2.1. *We can get the stability of the schemes by the structure-preserving results. Combining $\alpha, \beta > 0$ and $g > 0$, the definition of energy with the energy-preserving results $E^n = E^0$, we can obtain*

$$\max_{0 \le n \le N} \big\{\|u^n\|, \|u^n\|_1, \|\gamma^n\|, \|\gamma^n\|_1\big\} \le E^0,$$

where E^0 can be seen as a constant.

3. Analysis of Convergent Results

In the second section, a structure-preserving scheme is proposed based on the bi-variate function and the fully implicit method. The convergence order of the scheme will be concerned and rigorous analysis is given in this part.

Subtracting (2.6)-(2.8) from (2.3)-(2.5) and taking

$$e_j^n := U_j^n - u_j^n, \quad \eta_j^n := \Phi_j^n - \rho_j^n, \quad \bar{\eta}_j^n := \bar{\Phi}_j^n - \bar{\rho}_j^n,$$

we can get the error systems

$$\begin{aligned} &\delta_t e_j^{n+\frac{1}{2}} - \alpha \delta_t \varphi_2\big(e_j^{n+\frac{1}{2}}\big) + \psi\big(U^{n+\frac{1}{2}}, U^{n+\frac{1}{2}}\big)_j - \psi\big(u^{n+\frac{1}{2}}, u^{n+\frac{1}{2}}\big)_j \\ &\quad - \Big[\alpha\psi\big(\varphi_2(U^{n+\frac{1}{2}}), U^{n+\frac{1}{2}}\big)_j - \alpha\psi\big(\varphi_2(u^{n+\frac{1}{2}}), u^{n+\frac{1}{2}}\big)_j\Big] \\ &\quad + g\Phi_j^{n+\frac{1}{2}} \varphi_1\big(\bar{\Phi}_j^{n+\frac{1}{2}}\big) - g\rho_j^{n+\frac{1}{2}} \varphi_1\big(\bar{\rho}_j^{n+\frac{1}{2}}\big) = R_j^n, \end{aligned} \tag{3.1}$$

$$\delta_t \bar{\eta}_j^{n+\frac{1}{2}} - \beta \delta_t \varphi_2\big(\bar{\eta}_j^{n+\frac{1}{2}}\big) + \varphi_1\big(\Phi_j^{n+\frac{1}{2}} U_j^{n+\frac{1}{2}}\big) - \varphi_1\big(\rho_j^{n+\frac{1}{2}} u_j^{n+\frac{1}{2}}\big) = Q_j^n, \tag{3.2}$$

$$e_j^n = e_{j+M}^n, \quad \eta_j^n = \eta_{j+M}^n. \tag{3.3}$$

Assume the exact solutions satisfying $u(x,t) \in C^{5,3}(\mathbb{R}\times[0,T])$ and $\rho(x,t) \in C^{5,3}(\mathbb{R}\times[0,T])$ and define

$$C_u = \max_{0\le x\le L, 0\le t\le T}\{|u_t(x,t)|, |u(x,t)|, |u_x(x,t)|, |u_{xx}(x,t)|, |\rho(x,t)|, |\rho_x(x,t)|, |\rho_{xx}(x,t)|\}.$$

Based on the assumption and definition, we can derive the convergent conclusions.

Theorem 3.1. *Suppose that $U^n, \bar{\Phi}^n$ are the solution of (2.3)-(2.4) and $u^n, \bar{\rho}^n$ mean the approximation of them, there exists a positive constant h_0, when $\Delta t \le 1/(2c_2), \Delta h \le h_0$, we arrive at*

$$\|e^n\| \le c_3(\Delta t^2 + \Delta h^4), \quad \|e^n\|_1 \le c_3(\Delta t^2 + \Delta h^4), \tag{3.4}$$
$$\|\bar{\eta}^n\| \le c_3(\Delta t^2 + \Delta h^4), \quad \|\bar{\eta}^n\|_1 \le c_3(\Delta t^2 + \Delta h^4), \tag{3.5}$$

where

$$c_2 = \max\left\{2C_u + \frac{1}{4} + \frac{5\alpha}{4}C_u, \frac{C_u}{\alpha} + \frac{77C_u}{18}, \frac{C_u}{2\beta} + \frac{5C_u}{9} + \frac{5\alpha C_u}{4\beta}\right\}, \quad c_3 = \exp(c_2T)\frac{c_1^2}{c_2}.$$

Proof. Multiplying each side of (3.1) with $\Delta h e_j^{n+1/2}$ and summing the resulting equation over j from 1 to M, taking the definition of the inner product into account, we arrive at

$$\begin{aligned}
&\big(\delta_t e^{n+\frac{1}{2}}, e^{n+\frac{1}{2}}\big) - \alpha\big(\delta_t\varphi_2\big(e^{n+\frac{1}{2}}\big), e^{n+\frac{1}{2}}\big) + \big(\psi\big(U^{n+\frac{1}{2}}, U^{n+\frac{1}{2}}\big) - \psi\big(u^{n+\frac{1}{2}}, u^{n+\frac{1}{2}}\big), e^{n+\frac{1}{2}}\big)\\
&\quad - \big(\alpha\psi\big(\varphi_2(U^{n+\frac{1}{2}}), U^{n+\frac{1}{2}}\big) - \alpha\psi\big(\varphi_2(u^{n+\frac{1}{2}}), u^{n+\frac{1}{2}}\big), e^{n+\frac{1}{2}}\big)\\
&\quad + \big(g\Phi^{n+\frac{1}{2}}\varphi_1\big(\bar{\Phi}^{n+\frac{1}{2}}\big) - g\rho^{n+\frac{1}{2}}\varphi_1\big(\bar{\rho}^{n+\frac{1}{2}}\big), e^{n+\frac{1}{2}}\big) = \big(R^n, e^{n+\frac{1}{2}}\big).
\end{aligned} \tag{3.6}$$

In order to estimate the formulate step by step, we consider the facts that

$$\begin{aligned}
A :&= \psi\big(U^{n+\frac{1}{2}}, U^{n+\frac{1}{2}}\big) - \psi\big(u^{n+\frac{1}{2}}, u^{n+\frac{1}{2}}\big) = \psi\big(U^{n+\frac{1}{2}}, e^{n+\frac{1}{2}}\big) + \psi\big(e^{n+\frac{1}{2}}, u^{n+\frac{1}{2}}\big)\\
&= \psi\big(U^{n+\frac{1}{2}}, e^{n+\frac{1}{2}}\big) + \psi\big(e^{n+\frac{1}{2}}, u^{n+\frac{1}{2}}\big) - \psi\big(e^{n+\frac{1}{2}}, U^{n+\frac{1}{2}}\big) + \psi\big(e^{n+\frac{1}{2}}, U^{n+\frac{1}{2}}\big)\\
&= \psi\big(U^{n+\frac{1}{2}}, e^{n+\frac{1}{2}}\big) - \psi\big(e^{n+\frac{1}{2}}, e^{n+\frac{1}{2}}\big) + \psi\big(e^{n+\frac{1}{2}}, U^{n+\frac{1}{2}}\big),\\
B :&= \alpha\psi\big(\varphi_2(U^{n+\frac{1}{2}}), U^{n+\frac{1}{2}}\big) - \alpha\psi\big(\varphi_2\big(u^{n+\frac{1}{2}}\big), u^{n+\frac{1}{2}}\big)\\
&= \alpha\psi\big(\varphi_2(U^{n+\frac{1}{2}}), e^{n+\frac{1}{2}}\big) - \alpha\psi\big(\varphi_2(e^{n+\frac{1}{2}}), e^{n+\frac{1}{2}}\big) + \alpha\psi\big(\varphi_2\big(e^{n+\frac{1}{2}}\big), U^{n+\frac{1}{2}}\big),
\end{aligned} \tag{3.7}$$

$$\begin{aligned}
C :&= \Phi^{n+\frac{1}{2}}\varphi_1\big(\bar{\Phi}^{n+\frac{1}{2}}\big) - \rho^{n+\frac{1}{2}}\varphi_1\big(\bar{\rho}^{n+\frac{1}{2}}\big)\\
&= \Phi^{n+\frac{1}{2}}\varphi_1\big(\bar{\eta}^{n+\frac{1}{2}}\big) - \eta^{n+\frac{1}{2}}\varphi_1\big(\bar{\eta}^{n+\frac{1}{2}}\big) + \eta^{n+\frac{1}{2}}\varphi_1\big(\bar{\Phi}^{n+\frac{1}{2}}\big).
\end{aligned} \tag{3.8}$$

Combining the definition of $\psi(u,v)$ with (2.9), we can obtain

$$\begin{aligned}
\big(A, e^{n+\frac{1}{2}}\big) &= \big(\psi\big(e^{n+\frac{1}{2}}, U^{n+\frac{1}{2}}\big), e^{n+\frac{1}{2}}\big)\\
&= -\frac{1}{3}\big(e^{n+\frac{1}{2}}\big(U^{n+\frac{1}{2}}\big)_{\ddot{x}} + \big(e^{n+\frac{1}{2}}U^{n+\frac{1}{2}}\big)_{\ddot{x}}, e^{n+\frac{1}{2}}\big)\\
&\quad + \frac{4}{3}\big(e^{n+\frac{1}{2}}\big(U^{n+\frac{1}{2}}\big)_{\dot{x}} + \big(e^{n+\frac{1}{2}}U^{n+\frac{1}{2}}\big)_{\dot{x}}, e^{n+\frac{1}{2}}\big).
\end{aligned} \tag{3.9}$$

Applying Cauchy-Schwartz inequality, the regularity of the exact solution and (2.10), we get

$$\begin{aligned}
-\big((e^{n+\frac{1}{2}}U^{n+\frac{1}{2}})_{\dot{x}}, e^{n+\frac{1}{2}}\big) &= \big((e^{n+\frac{1}{2}})_{\dot{x}}U^{n+\frac{1}{2}}, e^{n+\frac{1}{2}}\big) + \big(e^{n+\frac{1}{2}}(U^{n+\frac{1}{2}})_{\dot{x}}, e^{n+\frac{1}{2}}\big) \\
&\le C_u\big(\|e^{n+\frac{1}{2}}\|^2 + \|e^{n+\frac{1}{2}}\|_1^2\big), \qquad (3.10)\\
-\big(e^{n+\frac{1}{2}}(U^{n+\frac{1}{2}})_{\dot{x}}, e^{n+\frac{1}{2}}\big) &\le C_u\|e^{n+\frac{1}{2}}\|^2, \qquad (3.11)\\
\big((e^{n+\frac{1}{2}}U^{n+\frac{1}{2}})_{\ddot{x}}, e^{n+\frac{1}{2}}\big) &\le C_u\big(\|e^{n+\frac{1}{2}}\|^2 + \|e^{n+\frac{1}{2}}\|_1^2\big), \qquad (3.12)\\
\big(e^{n+\frac{1}{2}}(U^{n+\frac{1}{2}})_{\ddot{x}}, e^{n+\frac{1}{2}}\big) &\le C_u\|e^{n+\frac{1}{2}}\|^2, \qquad (3.13)
\end{aligned}$$

where C_u depends on the regularity of the exact solution $U(t,x)$, which further implies that

$$-\big(\psi(e^{n+\frac{1}{2}}, U^{n+\frac{1}{2}}), e^{n+\frac{1}{2}}\big) \le \frac{10C_u}{3}\|e^{n+\frac{1}{2}}\|^2 + 3C_u\|e^{n+\frac{1}{2}}\|_1^2. \qquad (3.14)$$

Now, we estimate the second part by using (2.9),

$$\begin{aligned}
(B, e^{n+\frac{1}{2}}) &= \alpha\big(\psi(\varphi_2(e^{n+\frac{1}{2}}), U^{n+\frac{1}{2}}), e^{n+\frac{1}{2}}\big) + \alpha\big(\psi(\varphi_2(e^{n+\frac{1}{2}}), e^{n+\frac{1}{2}}), e^{n+\frac{1}{2}}\big)\\
&= \left[\frac{4\alpha}{3}\big(\varphi_2(e^{n+\frac{1}{2}})(U^{n+\frac{1}{2}})_{\dot{x}}, e^{n+\frac{1}{2}}\big) - \frac{\alpha}{3}\big(\varphi_2(e^{n+\frac{1}{2}})(U^{n+\frac{1}{2}})_{\ddot{x}}, e^{n+\frac{1}{2}}\big)\right]\\
&\quad + \left[\frac{4\alpha}{3}\big((\varphi_2(e^{n+\frac{1}{2}})U^{n+\frac{1}{2}})_{\dot{x}}, e^{n+\frac{1}{2}}\big) - \frac{\alpha}{3}\big((\varphi_2(e^{n+\frac{1}{2}})U^{n+\frac{1}{2}})_{\ddot{x}}, e^{n+\frac{1}{2}}\big)\right]\\
&= P_1 + P_2. \qquad (3.15)
\end{aligned}$$

Using the fact that

$$\varphi_1(u_j^n) = \frac{4}{3}(u_j^n)_{\dot{x}} - \frac{1}{3}(u_j^n)_{\ddot{x}}, \quad \varphi_2(u_j^n) = \frac{4}{3}(u_j^n)_{\bar{x}\bar{\bar{x}}} - \frac{1}{3}(u_j^n)_{\dot{x}\dot{x}},$$

and the property of $\varphi_2(u_j^n)$ presented in Lemma 2.1, we can get

$$\begin{aligned}
P_1 :&= \alpha\left(\varphi_2(e^{n+\frac{1}{2}})\left(\frac{4}{3}(U^{n+\frac{1}{2}})_{\dot{x}} - \frac{1}{3}(U^{n+\frac{1}{2}})_{\ddot{x}}\right), e^{n+\frac{1}{2}}\right)\\
&= \alpha\big(\varphi_1(U^{n+\frac{1}{2}})\varphi_2(e^{n+\frac{1}{2}}), e^{n+\frac{1}{2}}\big) = \alpha\big(\varphi_2(e^{n+\frac{1}{2}}), \varphi_1(U^{n+\frac{1}{2}})e^{n+\frac{1}{2}}\big)\\
&= -\frac{4\alpha}{3}\Big((e^{n+\frac{1}{2}})_{\bar{x}}, (\varphi_1(U^{n+\frac{1}{2}})e^{n+\frac{1}{2}})_{\bar{\bar{x}}}\Big) + \frac{\alpha}{3}\Big((e^{n+\frac{1}{2}})_{\dot{x}}, (\varphi_1(U^{n+\frac{1}{2}})e^{n+\frac{1}{2}})_{\dot{x}}\Big)\\
&= -\frac{4\alpha}{3}\sum_{j\in P_M}(e_j^{n+\frac{1}{2}})_{\bar{x}}\Big[\varphi_1(U_j^{n+\frac{1}{2}})e_j^{n+\frac{1}{2}} - \varphi_1(U_{j-1}^{n+\frac{1}{2}})e_{j-1}^{n+\frac{1}{2}}\Big]\\
&\quad + \frac{\alpha}{6}\sum_{j\in P_M}(e_j^{n+\frac{1}{2}})_{\dot{x}}\Big[\varphi_1(U_{j+1}^{n+\frac{1}{2}})e_{j+1}^{n+\frac{1}{2}} - \varphi_1(U_{j-1}^{n+\frac{1}{2}})e_{j-1}^{n+\frac{1}{2}}\Big]\\
&= -\frac{4\alpha}{3}\sum_{j\in P_M}\Big[\Delta h(e_j^{n+\frac{1}{2}})_{\bar{x}}\varphi_1(U_j^{n+\frac{1}{2}})(e_j^{n+\frac{1}{2}})_{\bar{\bar{x}}} + \Delta h(e_j^{n+\frac{1}{2}})_{\bar{x}}e_{j-1}^{n+\frac{1}{2}}\varphi_1(U_j^{n+\frac{1}{2}})_{\bar{\bar{x}}}\Big]\\
&\quad + \frac{\alpha}{12}\sum_{j\in P_M}\Big[\Delta h(e_j^{n+\frac{1}{2}})_{\dot{x}}^2\varphi_1(U_{j+1}^{n+\frac{1}{2}}) + \Delta h(e_j^{n+\frac{1}{2}})_{\dot{x}}e_{j-1}^{n+\frac{1}{2}}\varphi_1(U_{j+1}^{n+\frac{1}{2}})_{\dot{x}}\Big].
\end{aligned}$$

Together with the embedding inequality (2.10) and the definition of the norm, it infers that

$$P_1 \le \frac{17\alpha}{12}\|\varphi_1(U^{n+\frac{1}{2}})\|_\infty\Big(\|e^{n+\frac{1}{2}}\|\|e^{n+\frac{1}{2}}\|_1 + \|e^{n+\frac{1}{2}}\|_1^2\Big). \qquad (3.16)$$

Similarly, applying the property of integer established in Lemma 2.3, we arrive

$$\begin{aligned}P_2 &:= -\frac{4\alpha}{3}\Big(\varphi_2(e^{n+\frac{1}{2}})U^{n+\frac{1}{2}},(e^{n+\frac{1}{2}})_{\dot{x}}\Big)+\frac{\alpha}{3}\Big(\varphi_2(e^{n+\frac{1}{2}}U^{n+\frac{1}{2}}),(e^{n+\frac{1}{2}})_{\ddot{x}}\Big)\\ &= -\frac{16\alpha}{9}\Big((e^{n+\frac{1}{2}})_{\bar{x}\bar{\bar{x}}}U^{n+\frac{1}{2}},(e^{n+\frac{1}{2}})_{\dot{x}}\Big)+\frac{4\alpha}{9}\Big((e^{n+\frac{1}{2}})_{\dot{x}\dot{x}}U^{n+\frac{1}{2}},(e^{n+\frac{1}{2}})_{\dot{x}}\Big)\\ &\quad+\frac{4\alpha}{9}\Big((e^{n+\frac{1}{2}})_{\bar{x}\bar{\bar{x}}}U^{n+\frac{1}{2}},(e^{n+\frac{1}{2}})_{\ddot{x}}\Big)-\frac{\alpha}{9}\Big((e^{n+\frac{1}{2}})_{\dot{x}\dot{x}}U^{n+\frac{1}{2}},(e^{n+\frac{1}{2}})_{\ddot{x}}\Big)\\ &:= P_{21}+P_{22}+P_{23}+P_{24}.\end{aligned}$$

Actually, based on the period bounded condition, it can deduce that

$$\sum_{j=0}^{M}\Big[(e_j^{n+\frac{1}{2}})_{\bar{x}}^2-(e_{j-1}^{n+\frac{1}{2}})_{\bar{x}}^2\Big]=(e_M^{n+\frac{1}{2}})^2-(e_0^{n+\frac{1}{2}})^2=0.$$

Considering the grid function $\varphi_2(u_j^n)$ and the fact that

$$(u_j^n)_{\dot{x}}=\frac{1}{2}\Big((u_j^{n+\frac{1}{2}})_{\bar{x}}+(u_{j-1}^{n+\frac{1}{2}})_{\bar{x}}\Big),$$

we get

$$\begin{aligned}P_{21} &= -\frac{8\alpha}{9}\sum_{j\in P_M}U_j^{n+\frac{1}{2}}\Big[(e_j^{n+\frac{1}{2}})_{\bar{x}}-(e_{j-1}^{n+\frac{1}{2}})_{\bar{x}}\Big]\Big[(e_j^{n+\frac{1}{2}})_{\bar{x}}+(e_{j-1}^{n+\frac{1}{2}})_{\bar{x}}\Big]\\ &= -\frac{8\alpha}{9}\sum_{j\in P_M}U_j^{n+\frac{1}{2}}\Big[(e_j^{n+\frac{1}{2}})_{\bar{x}}^2-(e_{j-1}^{n+\frac{1}{2}})_{\bar{x}}^2\Big]\\ &= -\frac{8\alpha}{9}\sum_{j\in P_M}U_j^{n+\frac{1}{2}}(e_j^{n+\frac{1}{2}})_{\bar{x}}^2+\frac{8\alpha}{9}\sum_{j\in P_M}U_{j+1}^{n+\frac{1}{2}}(e_j^{n+\frac{1}{2}})_{\bar{x}}^2\\ &= \frac{8\alpha}{9}h\sum_{j\in P_M}(U_j^{n+\frac{1}{2}})_{\bar{x}}(e_j^{n+\frac{1}{2}})_{\bar{x}}^2\le\frac{8\alpha C_u}{9}\|e^{n+\frac{1}{2}}\|_1^2,\end{aligned}\tag{3.17}$$

$$P_{22}=\frac{2\alpha}{9}\Big[\sum_{j\in P_M}U_j^{n+\frac{1}{2}}(e_{j+1}^{n+\frac{1}{2}})_{\dot{x}}(e_j^{n+\frac{1}{2}})_{\dot{x}}-\sum_{j\in P_M}U_j^{n+\frac{1}{2}}(e_{j-1}^{n+\frac{1}{2}})_{\dot{x}}(e_j^{n+\frac{1}{2}})_{\dot{x}}\Big].\tag{3.18}$$

Using

$$\begin{aligned}&\sum_{j=0}^{M}U_j^{n+\frac{1}{2}}(e_{j-1}^{n+\frac{1}{2}})_{\dot{x}}(e_j^{n+\frac{1}{2}})_{\dot{x}}\\ &=\sum_{j=0}^{M}\Big[U_{j+1}^{n+\frac{1}{2}}(e_j^{n+\frac{1}{2}})_{\dot{x}}(e_{j+1}^{n+\frac{1}{2}})_{\dot{x}}+U_0^{n+\frac{1}{2}}(e_{M-1}^{n+\frac{1}{2}})_{\dot{x}}(e_0^{n+\frac{1}{2}})_{\dot{x}}-U_{M+1}^{n+\frac{1}{2}}(e_{M+1}^{n+\frac{1}{2}})_{\dot{x}}(e_M^{n+\frac{1}{2}})_{\dot{x}}\Big],\end{aligned}$$

Eq. (3.18) further gives that

$$\begin{aligned}P_{22} &= -\frac{2\alpha}{9}\Delta h\Big[\sum_{j\in P_M}(U_j^{n+\frac{1}{2}})_{\bar{x}}(e_{j+1}^{n+\frac{1}{2}})_{\dot{x}}(e_j^{n+\frac{1}{2}})_{\dot{x}}-\frac{2\alpha}{9}U_0^{n+\frac{1}{2}}(e_{M-1}^{n+\frac{1}{2}})_{\dot{x}}(e_0^{n+\frac{1}{2}})_{\dot{x}}\\ &\qquad-U_{M+1}^{n+\frac{1}{2}}(e_{M+1}^{n+\frac{1}{2}})_{\dot{x}}(e_M^{n+\frac{1}{2}})_{\dot{x}}\Big]\\ &\le\frac{4\alpha}{9}\|U^{n+\frac{1}{2}}\|_\infty\|e^{n+\frac{1}{2}}\|_1^2.\end{aligned}\tag{3.19}$$

It is time to give the estimation of P_{23}. Taking

$$\big(u_j^n\big)_{\ddot{x}} = \frac{1}{2}\big(\big(u_{j+1}^n\big)_{\dot{x}} + \big(u_{j-1}^n\big)_{\dot{x}}\big)$$

into account, we can obtain

$$\begin{aligned}
P_{23} &= \frac{\alpha}{9}\sum_{j\in P_M} U_j^{n+\frac{1}{2}}\Big[\big(e_j^{n+\frac{1}{2}}\big)_{\bar{x}} - \big(e_{j-1}^{n+\frac{1}{2}}\big)_{\bar{x}}\Big]\Big[\big(e_{j+1}^{n+\frac{1}{2}}\big)_{\dot{x}} + \big(e_{j-1}^{n+\frac{1}{2}}\big)_{\dot{x}}\Big]\\
&= \frac{\alpha}{18}\sum_{j\in P_M} U_j^{n+\frac{1}{2}}\Big[\big(e_j^{n+\frac{1}{2}}\big)_{\bar{x}} - \big(e_{j-1}^{n+\frac{1}{2}}\big)_{\bar{x}}\Big]\Big[\big(e_j^{n+\frac{1}{2}}\big)_{\bar{x}} + \big(e_{j-1}^{n+\frac{1}{2}}\big)_{\bar{x}}\Big]\\
&\quad + \frac{\alpha}{18}\sum_{j\in P_M} U_j^{n+\frac{1}{2}}\Big[\big(e_j^{n+\frac{1}{2}}\big)_{\bar{x}} - \big(e_{j-1}^{n+\frac{1}{2}}\big)_{\bar{x}}\Big]\Big[\big(e_{j+1}^{n+\frac{1}{2}}\big)_{\bar{x}} + \big(e_{j-2}^{n+\frac{1}{2}}\big)_{\bar{x}}\Big]\\
&= \frac{\alpha}{18}\sum_{j\in P_M} U_j^{n+\frac{1}{2}}\Big[\big(e_j^{n+\frac{1}{2}}\big)_{\bar{x}}\big(e_{j+1}^{n+\frac{1}{2}}\big)_{\bar{x}} - \big(e_{j-1}^{n+\frac{1}{2}}\big)_{\bar{x}}\big(e_{j-2}^{n+\frac{1}{2}}\big)_{\bar{x}}\Big]\\
&\quad + \frac{\alpha}{18}\sum_{j\in P_M} U_j^{n+\frac{1}{2}}\Big[\big(e_j^{n+\frac{1}{2}}\big)_{\bar{x}}\big(e_{j-2}^{n+\frac{1}{2}}\big)_{\bar{x}} - \big(e_{j-1}^{n+\frac{1}{2}}\big)_{\bar{x}}\big(e_{j+1}^{n+\frac{1}{2}}\big)_{\bar{x}}\Big]\\
&= -\frac{\alpha}{9}\sum_{j\in P_M} \Delta h\big(U_{j+1}^{n+\frac{1}{2}}\big)_{\dot{x}}\big(e_j^{n+\frac{1}{2}}\big)_{\bar{x}}\big(e_{j+1}^{n+\frac{1}{2}}\big)_{\bar{x}}\\
&\quad + \frac{\alpha}{18}\sum_{j\in P_M} \Delta h\big(U_j^{n+\frac{1}{2}}\big)_{\bar{x}}\big(e_j^{n+\frac{1}{2}}\big)_{\bar{x}}\big(e_{j-2}^{n+\frac{1}{2}}\big)_{\bar{x}}\\
&\le \frac{\alpha C_u}{6}\big\|e^{n+\frac{1}{2}}\big\|_1^2.
\end{aligned} \tag{3.20}$$

Using the same manner in the proof of P_{21} and (2.10), it is obvious that $P_{24} \le \alpha C_u\|e^{n+1/2}\|_1^2/36$.

Combining Eqs. (3.19) and (3.20), we can get

$$\big(B, e^{n+\frac{1}{2}}\big) \le \frac{55\alpha}{36}C_u\big\|e^{n+\frac{1}{2}}\big\|_1^2 + \frac{17\alpha}{12}\big\|\varphi_1\big(U^{n+\frac{1}{2}}\big)\big\|_\infty\Big(\big\|e^{n+\frac{1}{2}}\big\|\big\|e^{n+\frac{1}{2}}\big\|_1 + \big\|e^{n+\frac{1}{2}}\big\|_1^2\Big). \tag{3.21}$$

Before we give the estimation of (3.8), recalling the error equation (3.2) and taking inner product with $\bar{\eta}^{n+1/2}$ in each side, it arrives at

$$\begin{aligned}
&\big(\delta_t\bar{\eta}^{n+\frac{1}{2}}, \bar{\eta}^{n+\frac{1}{2}}\big) - \beta\big(\delta_t\varphi_2\big(\bar{\eta}^{n+\frac{1}{2}}\big), \bar{\eta}^{n+\frac{1}{2}}\big)\\
&\quad + \big(\varphi_1\big(\Phi^{n+\frac{1}{2}}U^{n+\frac{1}{2}}\big) - \varphi_1\big(\rho^{n+\frac{1}{2}}u^{n+\frac{1}{2}}\big), \bar{\eta}^{n+\frac{1}{2}}\big)\\
&= \big(Q^n, \bar{\eta}^{n+\frac{1}{2}}\big).
\end{aligned} \tag{3.22}$$

Applying the same manner of estimating A, we obtain

$$\begin{aligned}
D &:= -\varphi_1\big(\Phi^{n+\frac{1}{2}}U^{n+\frac{1}{2}}\big) + \varphi_1\big(\rho^{n+\frac{1}{2}}u^{n+\frac{1}{2}}\big)\\
&= -\varphi_1\big(\Phi^{n+\frac{1}{2}}e^{n+\frac{1}{2}}\big) + \varphi_1\big(\eta^{n+\frac{1}{2}}e^{n+\frac{1}{2}}\big) - \varphi_1\big(\eta^{n+\frac{1}{2}}U^{n+\frac{1}{2}}\big).
\end{aligned}$$

Together with Lemma 2.3 and Eq. (3.1), we can get

$$\begin{aligned}
&\frac{1}{\Delta t}\big[\big(\|e^{n+1}\|^2 - \|e^n\|^2\big) + \alpha\big(\|e^{n+1}\|_1^2 - \|e^n\|_1^2\big) + \big(\|\bar{\eta}^{n+1}\|^2 - \|\bar{\eta}^n\|^2\big) + \beta\big(\|\bar{\eta}^{n+1}\|_1^2 - \|\bar{\eta}^n\|_1^2\big)\big]\\
&= \big(-A + B, e^{n+\frac{1}{2}}\big) - \big(\varphi_1\big(\eta^{n+\frac{1}{2}}U^{n+\frac{1}{2}}\big), \bar{\eta}^{n+\frac{1}{2}}\big) - \big(\eta^{n+\frac{1}{2}}\varphi_1\big(\bar{\Phi}^{n+\frac{1}{2}}\big), e^{n+\frac{1}{2}}\big)\\
&\quad + \big(R^n, e^{n+\frac{1}{2}}\big) + \big(Q^n, \bar{\eta}^{n+\frac{1}{2}}\big).
\end{aligned} \tag{3.23}$$

Considering the equation $\rho = (1-\beta\partial_x^2)(\bar{\rho}-\rho_0)$, it is obvious that

$$\eta^{n+\frac{1}{2}} = \bar{\eta}^{n+\frac{1}{2}} - \beta\varphi_2\big(\bar{\eta}^{n+\frac{1}{2}}\big), \tag{3.24}$$

which further implies that

$$\begin{aligned}
&\big(\eta^{n+\frac{1}{2}}U^{n+\frac{1}{2}}, \varphi_1\big(\bar{\eta}^{n+\frac{1}{2}}\big)\big)\\
&= \big(\bar{\eta}^{n+\frac{1}{2}}U^{n+\frac{1}{2}}, \varphi_1\big(\bar{\eta}^{n+\frac{1}{2}}\big)\big) - \big(\beta\varphi_1\big(\bar{\eta}^{n+\frac{1}{2}}\big)U^{n+\frac{1}{2}}, \varphi_1\big(\bar{\eta}^{n+\frac{1}{2}}\big)\big)\\
&= \frac{4}{3}\Big(\bar{\eta}^{n+\frac{1}{2}}U^{n+\frac{1}{2}}, \big(\bar{\eta}^{n+\frac{1}{2}}\big)_{\dot{x}}\Big) - \frac{4\beta}{3}\Big(\varphi_2\big(\bar{\eta}^{n+\frac{1}{2}}\big)U^{n+\frac{1}{2}}, \big(\bar{\eta}^{n+\frac{1}{2}}\big)_{\dot{x}}\Big)\\
&\quad - \frac{1}{3}\Big(\bar{\eta}^{n+\frac{1}{2}}U^{n+\frac{1}{2}}, \big(\bar{\eta}^{n+\frac{1}{2}}\big)_{\ddot{x}}\Big) + \frac{\beta}{3}\Big(\varphi_2(\bar{\eta}^{n+\frac{1}{2}})U^{n+\frac{1}{2}}, (\bar{\eta}^{n+\frac{1}{2}})_{\ddot{x}}\Big) = \sum_{i=1}^{4} J_i.
\end{aligned} \tag{3.25}$$

Using the relation

$$(u_j^n)_{\ddot{x}} = \frac{1}{2}\Big(\big(u_{j+1}^n\big)_{\dot{x}} + \big(u_{j-1}^n\big)_{\dot{x}}\Big)$$

and the definition of the inner product, we arrive at

$$\begin{aligned}
J_1 + J_3 &= \frac{4}{3}\sum_{j\in P_M}\Delta h\bar{\eta}_j^{n+\frac{1}{2}}U_j^{n+\frac{1}{2}}\big(\bar{\eta}_j^{n+\frac{1}{2}}\big)_{\dot{x}}\\
&\quad - \frac{1}{3}\sum_{j\in P_M}\Delta h\bar{\eta}_j^{n+\frac{1}{2}}U_j^{n+\frac{1}{2}}\frac{\big(\bar{\eta}_{j-1}^{n+1/2}\big)_{\dot{x}} + \big(\bar{\eta}_{j-1}^{n+1/2}\big)_{\dot{x}}}{2}\\
&\le \big\|U^{n+\frac{1}{2}}\big\|_\infty\big\|\bar{\eta}^{n+\frac{1}{2}}\big\|_1\big\|\bar{\eta}^{n+\frac{1}{2}}\big\|.
\end{aligned} \tag{3.26}$$

We find that the way to estimate $J_2 + J_4$ is similar to P_2, thus we omit the details and directly give the result as

$$J_2 + J_4 \le \frac{5\beta C_u}{9}\big\|\bar{\eta}^{n+\frac{1}{2}}\big\|_1^2. \tag{3.27}$$

Similarly, we can get

$$-\big(\eta^{n+\frac{1}{2}}\varphi_1\big(\bar{\Phi}^{n+\frac{1}{2}}\big), e^{n+\frac{1}{2}}\big) \le \frac{15\alpha}{12}\big\|\varphi_1\big(\bar{\Phi}^{n+\frac{1}{2}}\big)\big\|_\infty\big(\big\|e^{n+\frac{1}{2}}\big\| + \big\|e^{n+\frac{1}{2}}\big\|_1\big)\big\|\bar{\eta}^{n+\frac{1}{2}}\big\|_1. \tag{3.28}$$

Substituting inequalities (3.9), (3.21) and (3.26)-(3.28) into (3.23), we can obtain

$$\begin{aligned}
&\frac{1}{\Delta t}\big[\big(\|e^{n+1}\|^2 - \|e^n\|^2\big) + \alpha\big(\|e^{n+1}\|_1^2 - \|e^n\|_1^2\big) + \big(\|\bar{\eta}^{n+1}\|^2 - \|\bar{\eta}^n\|^2\big) + \beta\big(\|\bar{\eta}^{n+1}\|_1^2 - \|\bar{\eta}^n\|_1^2\big)\big]\\
&\le 2C_u\big\|e^{n+\frac{1}{2}}\big\|^2 + C_u\big\|e^{n+\frac{1}{2}}\big\|_1^2 + \frac{17\alpha}{12}\big\|\varphi_1\big(U^{n+\frac{1}{2}}\big)\big\|_\infty\big(\big\|e^{n+\frac{1}{2}}\big\|\big\|e^{n+\frac{1}{2}}\big\|_1 + \big\|e^{n+\frac{1}{2}}\big\|_1^2\big)\\
&\quad + \frac{55\alpha}{36}C_u\big\|e^{n+\frac{1}{2}}\big\|_1^2 + \big\|U^{n+\frac{1}{2}}\big\|_\infty\big\|\bar{\eta}^{n+\frac{1}{2}}\big\|_1\big\|\bar{\eta}^{n+\frac{1}{2}}\big\| + \frac{5\beta C_u}{9}\big\|\bar{\eta}^{n+\frac{1}{2}}\big\|_1^2\\
&\quad + \frac{15\alpha}{12}\big\|\varphi_1\big(\bar{\Phi}^{n+\frac{1}{2}}\big)\big\|_\infty\big(\big\|e^{n+\frac{1}{2}}\big\| + \big\|e^{n+\frac{1}{2}}\big\|_1\big)\big\|\bar{\eta}^{n+\frac{1}{2}}\big\|_1 + \|R^n\|\big\|e^{n+\frac{1}{2}}\big\| + \|Q^n\|\big\|e^{n+\frac{1}{2}}\big\|.
\end{aligned} \tag{3.29}$$

Denoting

$$G^{n+1} = \|e^{n+1}\|^2 + \alpha\|e^{n+1}\|_1^2 + \|\bar{\eta}^{n+1}\|^2 + \beta\|\bar{\eta}^{n+1}\|_1^2,$$

and together with the assumption of the regularity of $U(x,t)$, we invert Eq. (3.29) into

$$\begin{aligned}\frac{G^{n+1}-G^n}{\Delta t} &\le \left(2C_u+\frac{5\alpha C_u}{4}+\frac{1}{4}\right)\left\|e^{n+\frac{1}{2}}\right\|^2+\left(C_u+\frac{77\alpha}{18}\right)\left\|e^{n+\frac{1}{2}}\right\|_1^2\\ &\quad+\frac{C_u}{2}\left\|\bar{\eta}^{n+\frac{1}{2}}\right\|^2+\left(\frac{C_u}{2}+\frac{5\beta C_u}{9}+\frac{5\alpha C_u}{24}\right)\left\|\bar{\eta}^{n+\frac{1}{2}}\right\|_1^2+\frac{c_1^2}{2}(\Delta t^2+\Delta h^4)^2\\ &\le c_2(G^n+G^{n+1})+\frac{c_1^2}{2}(\Delta t^2+\Delta h^4)^2, \end{aligned} \tag{3.30}$$

where

$$c_2=\max\left\{2C_u+\frac{1}{4}+\frac{5\alpha}{4}C_u,\frac{C_u}{\alpha}+\frac{77}{18},\frac{C_u}{2\beta}+\frac{5C_u}{9}+\frac{5\alpha C_u}{4\beta}\right\}.$$

Applying the discrete Grönwall inequality, when $\Delta t\le\tau_0=1/(2c_2)$, (3.30) implies that

$$G^{n+1}\le\exp(c_2T)\frac{c_1^2}{c_2}(\Delta t^2+\Delta h^4)^2.$$

Thus,

$$\begin{aligned}&\|e^{n+1}\|\le c_3(\Delta t^2+\Delta h^4),\quad \|e^{n+1}\|_1\le c_3(\Delta t^2+\Delta h^4),\\ &\|\bar{\eta}^{n+1}\|\le c_3(\Delta t^2+\Delta h^4),\quad \|\bar{\eta}^{n+1}\|_1\le c_3(\Delta t^2+\Delta h^4),\end{aligned}$$

where $c_3=\exp(c_2T)c_1^2/c_2$, which completes the proof. □

4. Numerical Experiments

In this section, several numerical experiments are given to show the correctness of our analysis, and we present the convergence order in L^2-norm in spatial direction and temporal direction, respectively. The momentum discrepancies Mo^n, the mass discrepancies Ma^n and the energy discrepancies D^n are defined as

$$Mo^n=\left|I_2^n-I_2^0\right|,\quad Ma^n=\left|I_1^n-I_1^0\right|,\quad D^n=|E^n-E^0|,\quad 1\le n\le N,$$

and when we choose the step size as Δh and Δt, the errors of u in space and time are defined as

$$\|F_1\|_1=\max_{0\le n\le N}\sqrt{\Delta h\sum_{j\in P_M}\left(-\varphi_2\big(u_j^n(\Delta h,\Delta t)\big)u_j^n(\Delta h,\Delta t)+\varphi_2\left(u_{2j}^n\left(\frac{\Delta h}{2},\Delta t\right)\right)u_{2j}^n\left(\frac{\Delta h}{2},\Delta t\right)\right)},$$

$$\|G_1\|_1=\max_{0\le n\le N}\sqrt{\Delta h\sum_{j\in P_M}\left(-\varphi_2\big(u_j^n(\Delta h,\Delta t)\big)u_j^n(\Delta h,\Delta t)+\varphi_2\left(u_j^{2n}\left(\Delta h,\frac{\Delta t}{2}\right)\right)u_j^{2n}\left(\Delta h,\frac{\Delta t}{2}\right)\right)},$$

$$\|F_1\|=\max_{0\le n\le N}\sqrt{\Delta h\sum_{j\in P_M}\left|u_j^n(\Delta h,\Delta t)-u_{2j}^n\left(\frac{\Delta h}{2},\Delta t\right)\right|^2},$$

$$\|G_1\|=\max_{0\le n\le N}\sqrt{\Delta h\sum_{j\in P_M}\left|u_j^n(\Delta h,\Delta t)-u_j^{2n}\left(\Delta h,\frac{\Delta t}{2}\right)\right|^2},$$

and $\|F_2\|_1, \|G_2\|_1, \|F_2\|, \|G_2\|$ are defined similarly for $\bar{\rho}$. In order to ignore the impact of time step sizes on calculation results, we give the definition of the error in L^∞-norm as

$$\|F_1\|_{L^\infty} = \max_{0\le n\le N, j\in P_M} \left\| u_j^n(\Delta h, \Delta t) - u_{2j}^{4n}\left(\frac{\Delta h}{2}, \frac{\Delta t}{4}\right)\right\|,$$
$$\|F_2\|_{L^\infty} = \max_{0\le n\le N, j\in P_M} \left\| \bar{\rho}_j^n(\Delta h, \Delta t) - \bar{\rho}_{2j}^{4n}\left(\frac{\Delta h}{2}, \frac{\Delta t}{4}\right)\right\|.$$

We test the errors in L^∞-norm in spatial direction, while simultaneously refining both the spatial step Δh and time step Δt. This coupled refinement strategy ensures that the discretization error in temporal direction does not dominate the results, allowing us to isolate and properly assess the spatial convergence properties of the scheme. Moreover, by using the following condition:

$$\mathcal{O}\left(\left(\frac{\Delta h}{2}\right)^4 + \left(\frac{\Delta t}{4}\right)^2\right) = \frac{1}{16}\mathcal{O}(\Delta h^4 + \Delta t^2),$$

the spatial convergence orders of u can be defined for sufficiently small Δh and Δt as

$$\text{order}_u^\infty = \log \frac{\|F_1(\Delta h, \Delta t)\|_{L^\infty}}{\|F_1(\Delta h/2, \Delta t/4)\|_{L^\infty}}, \quad \text{order}_p^\infty = \log \frac{\|F_2(\Delta h, \Delta t)\|_{L^\infty}}{\|F_2(\Delta h/2, \Delta t/4)\|_{L^\infty}}. \tag{4.1}$$

Example 4.1. Consider the dark break problems [49] with periodic boundary conditions first. The dam-break initial conditions are

$$\bar{\rho}_0(x) = 1 + \tanh(x + a) - \tanh(x - a), \quad u_0(x) = 0, \quad x \in [-L, L],$$

where a represents the dam-breaking parameter.

Case 1. We choose $g = 1, \alpha = 0.8, \beta = 0.2, a = 4, \bar{\rho}_0 = 0$ on the periodic domain $(x, t) \in [-12\pi, 12\pi] \times (0, 1]$.

The errors and convergence orders of u and ρ in spatial direction are shown in Table 4.1, where we refine the spatial step size with a fixed temporal step-size $\Delta t = 1/1000$. The errors and convergence orders in temporal direction are shown in Table 4.2, where we refine the temporal step size with a fixed spatial step-size $\Delta h = 3\pi/125$. The convergence rates of scheme (3.1) and (3.2) can reach 2 order in the temporal direction and 4 order in the spatial direction. Moreover, we simulate the schemes where both the temporal step size Δt and spatial mesh size Δh are reduced. Table 4.3 declares that the schemes achieve fourth order in space. The numerical results are consistent with our theoretical results.

Moreover, we present the mass-, energy- and momentum-conservation properties of the numerical scheme (2.6)-(2.8) in Fig. 4.1, where we contrast our present method with a linearized

Table 4.1: Spatial convergence rates with $\Delta t = 1/1000$ of Case 1.

Δh	$\|F_1\|_1$	order_u^1	$\|F_1\|$	order_u^2	$\|F_2\|_1$	order_p^1	$\|F_2\|$	order_p^2
1/5	2.80e-03	*	9.01e-04	*	2.94e-03	*	8.90e-04	*
1/10	1.99e-04	3.81	6.05e-05	3.90	2.09e-04	3.81	5.98e-05	3.90
1/20	1.28e-05	3.96	3.85e-06	3.97	1.35e-05	3.95	3.81e-06	3.97
1/40	8.07e-07	3.99	2.42e-07	3.99	8.50e-07	3.99	2.39e-07	3.99

Table 4.2: Temporal convergence rates with $\Delta h = 3\pi/125$ of Case 1.

Δt	$\|G_1\|_1$	order_u^1	$\|G_1\|$	order_u^2	$\|G_2\|_1$	order_p^1	$\|G_2\|$	order_p^2
1/16	1.90e-03	*	1.21e-03	*	2.00e-03	*	1.20e-03	*
1/32	4.78e-04	1.99	3.03e-04	1.99	5.03e-04	1.99	3.03e-04	1.99
1/64	1.20e-04	2.00	7.59e-05	2.00	1.26e-04	2.00	7.57e-05	2.00
1/128	3.00e-05	2.00	1.90e-05	2.00	3.15e-05	2.00	1.89e-05	2.00

Table 4.3: Spatial convergence rates with different Δh of Case 1.

Δh	Δt	$\|F_1\|_{L^\infty}$	order_u^∞	$\|F_2\|_{L^\infty}$	order_p^∞
1/5	1/10	2.90e-03	*	3.06e-03	*
1/10	1/40	1.92e-04	3.91	2.04e-04	3.91
1/20	1/160	1.23e-05	3.97	1.29e-05	3.97
1/40	1/640	7.71e-07	4.00	8.06e-07	4.00

Euler method in [13]. The time domain is chosen as $[0, 50]$, the step sizes are defined as $\Delta t = 1/10, \Delta h = \pi/25$. We denote "Ma-E, Mo-E, D-E" as the evolution of three invariants of the Euler method, and "Ma-I, Mo-I, D-I" as the evolution of three invariants of our present method. Our numerical schemes can preserve the energy, mass and momentum discrete conservation law, which agrees with our theoretical analysis.

We simulate the long-term behavior of the two-component Euler-Poincaré equations in Fig. 4.2 with $T = 50, \Delta h = \pi/20, \Delta t = 1/50$. We can find that the amplitude of the numerical solutions comes to zero at the moment of overlap, accompanied by a vertical slope. Subsequently, peaks emerge and subsequently recede as time progresses. Such performance matches with the conclusion in [49].

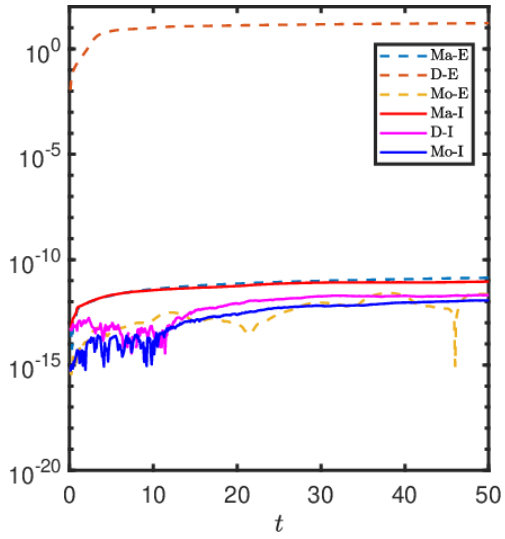

Fig. 4.1. Evolution of D^n, Ma^n, Mo^n for the different discrete schemes for $\Delta t = 1/10, \Delta h = 3\pi/50$ of Case 1.

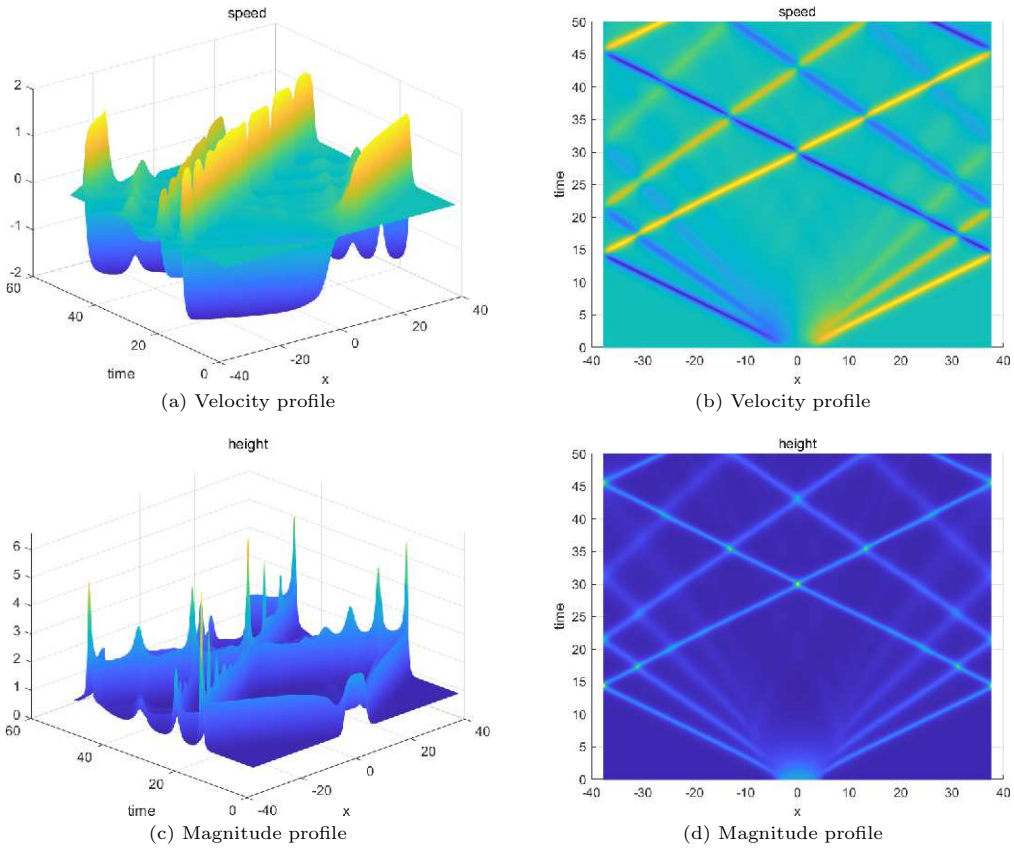

(a) Velocity profile (b) Velocity profile

(c) Magnitude profile (d) Magnitude profile

Fig. 4.2. The simulated profiles of the velocity $u(x,t)$ and the magnitude $\rho(x,t)$ at two view angles in Case 1.

Case 2. We choose $g = 1, \alpha = 0.3, \beta = 1, a = 0.2, \bar{\rho}_0 = 0$ on the periodic domain $(x,t) \in [-8,8] \times (0,1]$.

The errors and convergence orders of u and ρ in spatial direction are shown in Table 4.4, where we refine the spatial step size with a fixed temporal step-size $\Delta t = 1/1000$. The errors and convergence orders in temporal direction are shown in Table 4.5, where we refine the temporal step size with a fixed spatial step-size $\Delta h = 1/100$. The results present that the convergence rates for both velocity and magnitude are 2-order in time and 4-order in space. Similarly, Table 4.6 demonstrates that the spatial error estimations are fourth order. The numerical results match our theoretical results ideally.

Table 4.4: Spatial convergence rates with $\Delta t = 1/1000$ of Case 2.

Δh	$\|F_1\|_1$	order_u^1	$\|F_1\|$	order_u^2	$\|F_2\|_1$	order_p^1	$\|F_2\|$	order_p^2
16/100	5.02e-04	*	1.09e-04	*	2.40e-04	*	6.96e-05	*
16/200	3.42e-05	3.87	7.23e-06	3.91	1.59e-05	3.93	4.53e-06	3.94
16/400	2.19e-06	3.97	4.60e-07	3.98	1.01e-06	3.98	2.86e-07	3.98
16/800	1.37e-07	4.00	2.89e-08	3.99	6.29e-08	4.00	1.79e-08	4.00

Table 4.5: Temporal convergence rates with $\Delta h = 1/100$ of Case 2.

Δt	$\|G_1\|_1$	order_u^1	$\|G_1\|$	order_u^2	$\|G_2\|_1$	order_p^1	$\|G_2\|$	order_p^2
1/8	3.64e-06	*	1.20e-05	*	5.17e-06	*	1.07e-06	*
1/16	9.10e-07	2.00	3.01e-06	2.00	1.29e-06	2.00	2.67e-07	2.00
1/32	2.28e-07	2.00	7.53e-07	2.00	3.23e-07	2.00	6.67e-08	2.00
1/64	5.69e-08	2.00	1.88e-07	2.00	8.09e-08	2.00	1.67e-08	2.00

Table 4.6: Spatial convergence rates with different Δh of Case 2.

Δh	Δt	$\|F_1\|_{L^\infty}$	order_u^1	$\|F_2\|_{L^\infty}$	order_p^1
32/100	1/10	6.60e-04	*	4.33e-04	*
32/200	1/40	5.50e-05	3.59	3.38e-05	3.68
32/400	1/160	3.75e-06	3.87	2.29e-06	3.88
32/800	1/640	2.40e-07	3.97	1.46e-07	3.97

Moreover, we present the mass-, energy- and momentum-conservation properties of the numerical scheme (2.6)-(2.8) in Fig. 4.3, where we contrast our present method with a Linearize Euler method. We denote "Ma-E, Mo-E, D-E" as the evolution of three invariants of the Euler method, and "Ma-I, Mo-I, D-I" as the evolution of three invariants of our present method. The evolutions of three invariants are presented in the time domain $[0, 100]$, and the step sizes are chosen as $\Delta t = 1/20,\ \Delta h = 1/20$. The result is consist with our analysis.

The long-term simulation is presented in Fig. 4.4 with $T = 100, \Delta h = 16/100, \Delta t = 1/50$. The periodicity as well as the symmetry of the waveforms can be well observed. Such performance also matches with the conclusion in [49].

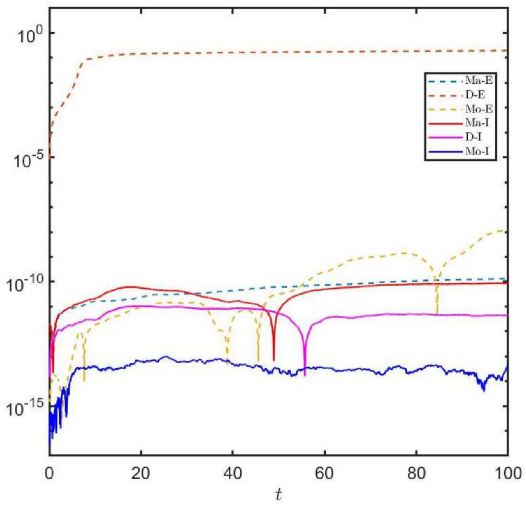

Fig. 4.3. Evolution of D^n, Ma^n, Mo^n for the different discrete schemes for $\Delta t = 1/20, \Delta h = 1/20$.

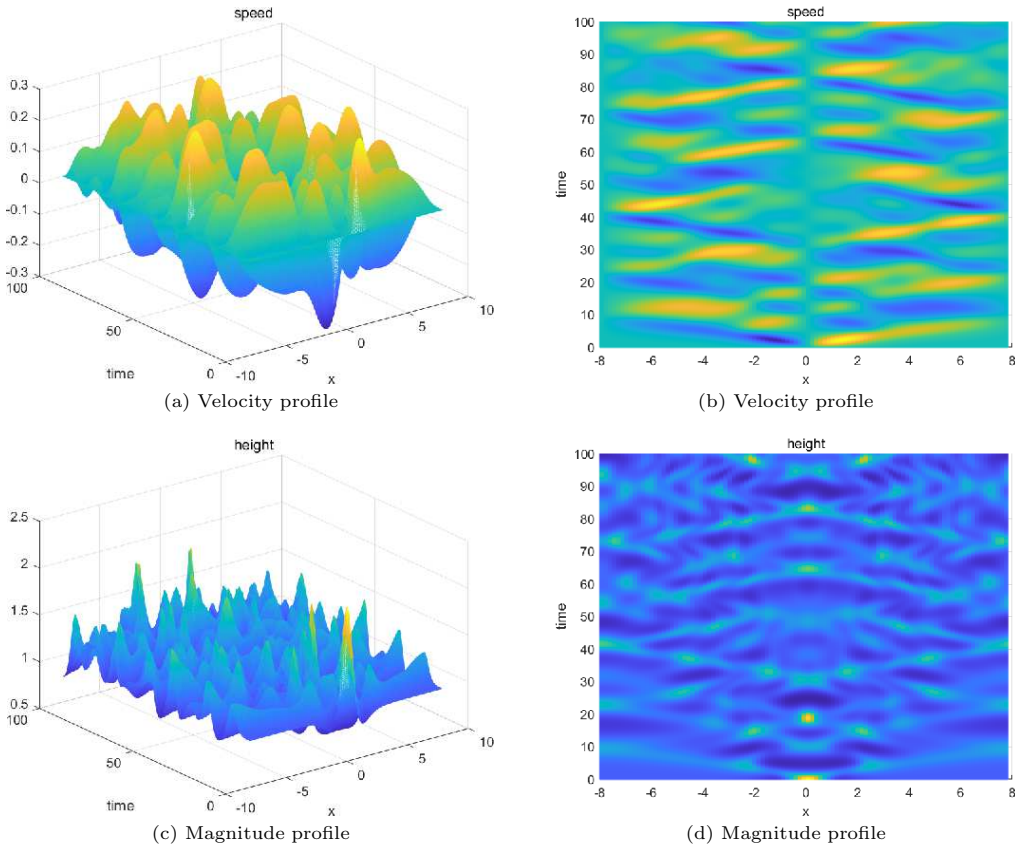

(a) Velocity profile (b) Velocity profile

(c) Magnitude profile (d) Magnitude profile

Fig. 4.4. The simulated profiles of the velocity $u(x,t)$ and the magnitude $\rho(x,t)$ at two view angles in Case 2.

Example 4.2. We consider a solitary wave propagation problem with the following initial data:

$$u_0(x) = \frac{\sqrt{g}}{10}\,\mathrm{sech}^2\left(\sqrt{\frac{3}{40}}(x-70)\right),$$
$$\bar{\rho}_0(x) = 1 + \frac{1}{10}\,\mathrm{sech}^2\left(\sqrt{\frac{3}{40}}(x-70)\right),$$

where we choose $\alpha = 0.6, \beta = 0.2, g = 9.81, \bar{\rho}_0 = 0$. The spatial domain is chosen as $x \in [0, 200]$.

We present the errors of u and ρ in spatial direction and temporal direction in Tables 4.7 and 4.8, respectively. We fix the temporal step size as $\Delta t = 1/1000$ to calculate the convergence

Table 4.7: Spatial convergence rates with $\Delta t = 1/1000$ of Example 4.2.

Δh	$\|F_1\|_1$	order_u^1	$\|F_1\|$	order_u^2	$\|F_2\|_1$	order_p^1	$\|F_2\|$	order_p^2
1	2.93e-03	*	2.93e-03	*	1.05e-03	*	1.01e-03	*
1/2	2.16e-04	3.76	2.06e-04	3.83	7.90e-05	3.73	7.21e-05	3.81
1/4	1.40e-05	3.94	1.32e-05	3.96	5.15e-06	3.94	4.65e-06	3.95
1/8	8.85e-07	3.99	8.33e-07	3.99	3.26e-07	3.99	2.93e-07	3.99

Table 4.8: Temporal convergence rates with $\Delta h = 1/10$ of Example 4.2.

Δt	$\|G_1\|_1$	order_u^1	$\|G_1\|$	order_u^2	$\|G_2\|_1$	order_p^1	$\|G_2\|$	order_p^2
1/8	1.27e-03	*	1.71e-03	*	4.27e-04	*	5.58e-04	*
1/16	3.23e-04	1.98	4.33e-04	1.98	1.09e-04	1.98	1.41e-04	1.98
1/32	8.11e-05	1.99	1.09e-04	2.00	2.73e-05	1.99	3.54e-05	2.00
1/64	2.03e-05	2.00	2.72e-05	2.00	6.83e-06	2.00	8.86e-06	2.00

rates in space, which can reach 4 order. Simultaneously, we fix the spatial step size as $\Delta h = 1/10$ to calculate the convergence rates in time, which can reach 2 order. Such numerical results are consistent with the theoretical convergence results.

Then, we contrast the scheme (2.6)-(2.7) with a linearized Euler method, where we define $\Delta h = 1, \Delta t = 1/20, T = 100$. The evolutions of discrepancies of mass, momentum, energy are shown in Fig. 4.5. We can find that the scheme can preserve three invariants during a long time simulation. Furthermore, the propagation of the velocity and magnitude of the wave are presented in Fig. 4.6 with $T = 100, \Delta h = 1, \Delta t = 1/50$. The waveforms presented by the numerical solutions are observed from two different angles. The periodicity results are in agreement with the conclusion in [8].

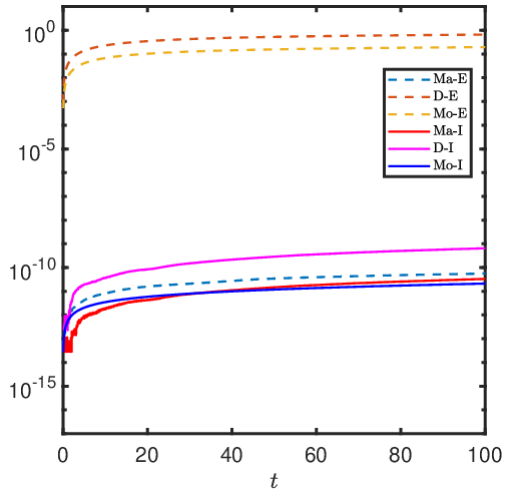

Fig. 4.5. Evolution of D^n, Ma^n, Mo^n for the different discrete schemes for $\Delta t = 1/50, \Delta h = 1$ of Example 4.2.

5. Conclusion

In this paper, we propose a multiple-invariants preserving numerical scheme for the MEP2. The scheme is proved to preserve mass, energy and momentum discretely. Moreover, the numerical experiments show that the scheme can reach fourth order in spatial direction and second order in temporal direction. Several experiments are shown the consistence between the numerical results and the theoretical analysis.

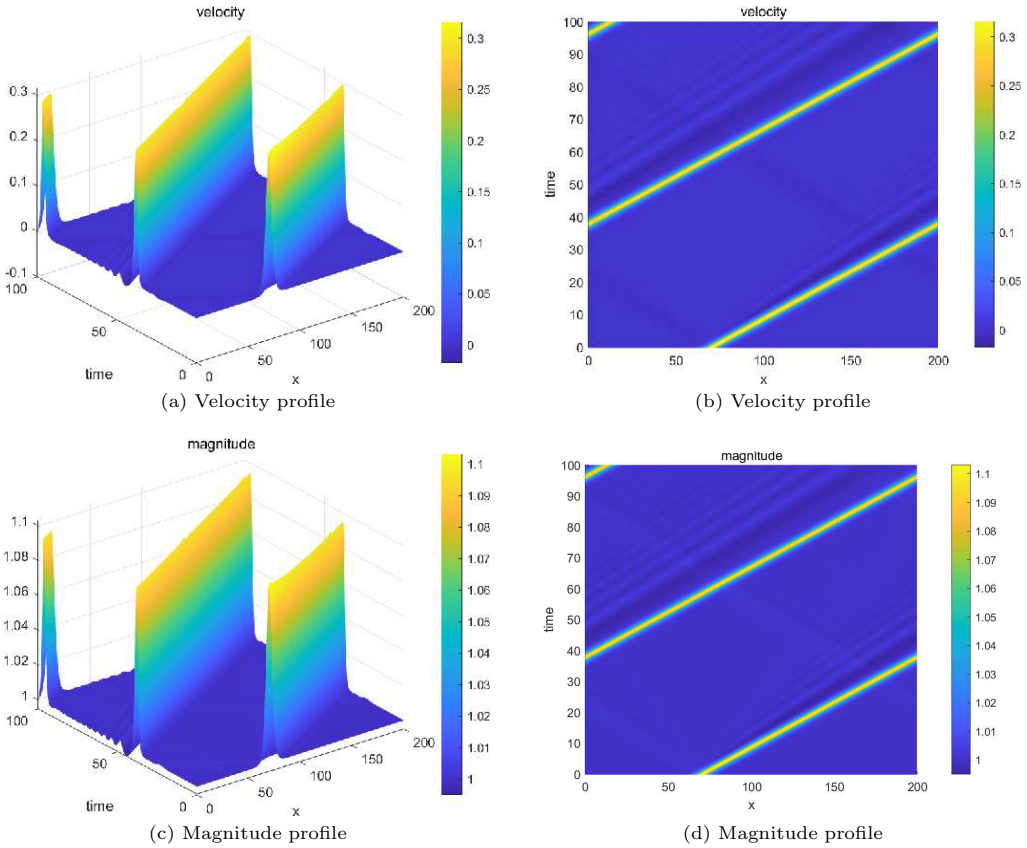

(a) Velocity profile (b) Velocity profile

(c) Magnitude profile (d) Magnitude profile

Fig. 4.6. The simulated profiles of the velocity $u(x,t)$ and the magnitude $\rho(x,t)$ at two view angles in Example 4.2.

Appendix A

In this section, the implement of our methods is presented. Suppose the numerical solutions of $u_i^k, \rho_i^k, \bar{\rho}_i^k, i \in P_M, 0 \le k \le n-1$ have been calculated, we now compute the solutions at $t = n\Delta t$.

We define the iteration number of predictor-corrector method as l. Let the l-th predict numerical solution of u_j^n, ρ_j^n be $\tilde{u}_j^{n,l}, \tilde{\rho}_j^{n,l}$ and $u_j^{n+1} = \tilde{u}_j^{n+1,l_m}$ and $\tilde{\bar{\rho}}_j^{n+1} = \tilde{\bar{\rho}}_j^{n+1,l_m}$, where l_m means the steps of iteration and $l = 1, 2, \ldots, l_m$. Suppose we have calculated $\tilde{u}_j^{n+1,l}$ and define $\tilde{u}_j^{n+1/2,l} = (\tilde{u}_j^{n+1,l} + u_j^n)/2$, we compute the $(l+1)$-th iteration numerical solutions $\tilde{u}_j^{n+1,l+1}$ and $\tilde{\bar{\rho}}_j^{n+1,l+1}$ by calculating $\tilde{u}_j^{n+1/2,l+1}$ and $\tilde{\bar{\rho}}_j^{n+1/2,l+1}$ as following:

$$
\begin{aligned}
&\frac{1}{\Delta t}\big(\tilde{u}_j^{n+1,l+1} - u_j^n\big) - \frac{\alpha}{\Delta t}\big(\varphi_2\big(\tilde{u}_j^{n+1,l+1}\big) - \varphi_2\big(u_j^n\big)\big) \\
&\quad + \frac{4}{3}\left(\frac{\tilde{u}_j^{n+1/2,l} + \tilde{u}_{j+1}^{n+1/2,l}}{2\Delta h}\tilde{u}_{j+1}^{n+\frac{1}{2},l+1} - \frac{\tilde{u}_j^{n+1/2,l} + \tilde{u}_{j-1}^{n+1/2,l}}{2\Delta h}\tilde{u}_{j-1}^{n+\frac{1}{2},l+1}\right) \\
&\quad - \frac{1}{3}\left(\frac{\tilde{u}_j^{n+1/2,l} + \tilde{u}_{j+2}^{n+1/2,l}}{4\Delta h}\tilde{u}_{j+2}^{n+\frac{1}{2},l+1} - \frac{\tilde{u}_j^{n+1/2,l} + \tilde{u}_{j-2}^{n+1/2,l}}{4\Delta h}\tilde{u}_{j-2}^{n+\frac{1}{2},l+1}\right)
\end{aligned}
$$

$$
\begin{aligned}
&- \frac{4\alpha}{3}\left(\frac{\varphi_2(\tilde{u}_j^{n+1/2,l})+\varphi_2(\tilde{u}_{j+1}^{n+1/2,l})}{2\Delta h}\tilde{u}_{j+1}^{n+\frac{1}{2},l+1} - \frac{\varphi_2(\tilde{u}_j^{n+1/2,l})+\varphi_2(\tilde{u}_{j-1}^{n+1/2,l})}{2\Delta h}\tilde{u}_{j-1}^{n+\frac{1}{2},l+1}\right)\\
&- \frac{\alpha}{3}\left(\frac{\varphi_2(\tilde{u}_j^{n+1/2,l})+\varphi_2(\tilde{u}_{j+2}^{n+1/2,l})}{4\Delta h}\tilde{u}_{j+2}^{n+\frac{1}{2},l+1} - \frac{\varphi_2(\tilde{u}_j^{n+1/2,l})+\varphi_2(\tilde{u}_{j-2}^{n+1/2,l})}{4\Delta h}\tilde{u}_{j-2}^{n+\frac{1}{2},l+1}\right)\\
&+ g\left(\frac{2\tilde{\rho}_j^{n+1/2,l}}{3\Delta h}\tilde{\bar{\rho}}_{j+1}^{n+\frac{1}{2},l+1} - \frac{2\tilde{\rho}_j^{n+1/2,l}}{3\Delta h}\tilde{\bar{\rho}}_{j-1}^{n+\frac{1}{2},l+1}\right.\\
&\qquad\left. - \frac{\tilde{\rho}_j^{n+1/2,l}}{12\Delta h}\tilde{\bar{\rho}}_{j+2}^{n+\frac{1}{2},l+1} + \frac{\tilde{\rho}_j^{n+1/2,l}}{12\Delta h}\tilde{\bar{\rho}}_{j-2}^{n+\frac{1}{2},l+1}\right) = 0, \qquad \text{(A.1)}
\end{aligned}
$$

$$
\begin{aligned}
&\frac{1}{\Delta t}\big(\tilde{\bar{\rho}}_j^{n+1,l+1} - \bar{\rho}_j^n\big) - \frac{\beta}{\Delta t}\big(\varphi_2\big(\tilde{\bar{\rho}}_j^{n+1,l+1}\big) - \varphi_2\big(\bar{\rho}_j^n\big)\big)\\
&+ \left(\frac{2\tilde{\rho}_{j+1}^{n+1/2,l}}{3\Delta h}\tilde{u}_{j+1}^{n+\frac{1}{2},l+1} - \frac{2\tilde{\rho}_{j-1}^{n+1/2}}{3\Delta h}\tilde{u}_{j-1}^{n+\frac{1}{2},l+1}\right.\\
&\qquad\left. - \frac{\tilde{\rho}_{j+2}^{n+1/2,l}}{12\Delta h}\tilde{u}_{j+2}^{n+\frac{1}{2},l+1} - \frac{\tilde{\rho}_{j-2}^{n+1/2,l}}{12\Delta h}\tilde{u}_{j-2}^{n+\frac{1}{2},l+1}\right), \qquad \text{(A.2)}
\end{aligned}
$$

where

$$
\tilde{u}_j^{n+1,l+1} = 2\tilde{u}_j^{n+\frac{1}{2},l+1} - u_j^n, \quad \tilde{\bar{\rho}}_j^{n+1,l+1} = 2\bar{\rho}_j^{n+\frac{1}{2},l+1} - \bar{\rho}_j^n.
$$

Then we can calculate the $\tilde{\rho}_j^{n+1/2,l+1}$ by

$$
\tilde{\rho}_j^{n+1,l+1} = (\tilde{\bar{\rho}}_j^{n+1,l+1} - \rho_0) - \beta\varphi_2(\tilde{\bar{\rho}}_j^{n+1,l+1}). \qquad \text{(A.3)}
$$

The detailed algorithm flow chart is listed in Algorithm A.1.

Algorithm A.1: The Calculation Process of Numerical Scheme (2.6)-(2.7).

1 Suppose $u_j^{n+1,0}, \rho_j^{n+1,0}, \bar{\rho}_j^{n+1,0} = u_j^n, \rho_j^n, \bar{\rho}_j^n$.
2 Suppose the tolerance error $\epsilon = 1$.
3 Set the iteration number $l = 1$.
4 **while** $(\epsilon > 10^{-10})$ or $(l < 50)$ **do**
5 Let $\tilde{u}_j^{n+1/2,l} = (u_j^n + \tilde{u}_j^{n+1,l})/2$.
6 Calculate $\tilde{u}_j^{n+1,l+1}$ and $\tilde{\bar{\rho}}_j^{n+1,l+1}$ by using (A.1) and (A.2).
7 Calculate $\tilde{\rho}_j^{n+1/2,l+1}$ by using (A.3).
8 Calculate $\epsilon = \max_{j\in P_M}\{|\tilde{u}_j^{n+1/2,l+1} - \tilde{u}_j^{n+1/2,l}|, |\tilde{\bar{\rho}}_j^{n+1/2,l+1} - \tilde{\bar{\rho}}_j^{n+1/2,l}|\}$.
9 Update the iteration number $l = l + 1$.
10 **end**

Acknowledgements. The research was supported by the Guangdong Basic and Applied Basic Research Foundation (Grant Nos. 2023A1515111169, 2024A1515011883), by the National Natural Science Foundation of China (Grant Nos. 11771162, 12231003), by the Zhejiang Provincial Natural Science Foundation of China (Grant No. LZ23A010007).

References

[1] G. Akrivis and D. Li, Structure-preserving Gauss methods for the nonlinear Schrödinger equation, *Calcolo*, **58**:2 (2011), 1–25.

[2] A. Bressan and A. Constantin, Global conservative solutions of the Camassa-Holm equation, *Arch. Ration. Mech. Anal.*, **183** (2007), 215–239.

[3] R.K. Bullough, "The wave" "par excellence", the solitary progressive great wave of equilibrium of the fluid: An early history of the solitary wave, in: *Solitons. Springer Series in Nonlinear Dynamics*, Springer, (1988), 7–42.

[4] R. Camassa and D.D. Holm, An integrable shallow water equation with peaked solitons, *Phys. Rev. Lett.*, **71** (1993), 1661–1664.

[5] W. Cao, D. Li, and Z. Zhang, Unconditionally optimal convergence of an energy-conserving and linearly implicit scheme for nonlinear wave equations, *Sci. China Math.*, **65** (2022), 1731–1748.

[6] D. Caviedes-Voullième, J. Fernández-Pato, and C. Hinz, Performance assessment of 2D zero-inertia and shallow water models for simulating rainfall-runoff processes, *J. Hydrol.*, **584** (2020), 124663.

[7] M. Chen, S.Q. Liu, and Y. Zhang, A two-component generalization of the Camassa-Holm equation and its solutions, *Lett. Math. Phys.*, **75** (2006), 1–15.

[8] A. Chertock, A. Kurganov, and Y. Liu, Finite-volume-particle methods for the two-component Camassa-Holm system, *Commun. Comput. Phys.*, **27**:2 (2019), 480–502.

[9] G.M. Coclite, K.H. Karlsen, and N.H. Risebro, A convergent finite difference scheme for the Camassa-Holm equation with general H^1 initial data, *SIAM J. Numer. Anal.*, **46**:3 (2008), 1154–1579.

[10] A. Constantin and R.I. Ivanov, On an integrable two-component Camassa-Holm shallow water system, *Phys. Lett. A*, **372** (2008), 7129–7132.

[11] J. Escher, O. Lechtenfeld, and Z. Yin, Well-posedness and blow-up phenomena for the 2-component Camassa-Holm equation, *Discrete Contin. Dyn. Syst.*, **19** (2007), 493–513.

[12] G. Falqui, On a Camassa-Holm type equation with two dependent variables, *J. Phys. A: Math. Gen.*, **39** (2006), 327–342.

[13] R. Gao, D. Li, M. Mei, and D. Zhao, A decoupled, linearly implicit and high-order structure-preserving scheme for Euler-Poincaré equations, *Math. Comput. Simulation*, **218** (2024), 679–703.

[14] P. García-Navarro, J. Murillo, J. Fernández-Pato, I. Echeverribar, and M. Morales-Hernández, The shallow water equations and their application to realistic cases, *Environ. Fluid Mech.*, **19** (2019), 1235–1252.

[15] A. Ghiloufi and K. Omrani, New conservative difference schemes with fourth-order accuracy for some model equation for nonlinear dispersive waves, *Numer. Methods Partial Differential Equations*, **34** (2018), 451–500.

[16] W. Hereman, Shallow water waves and solitary waves, in: *Encyclopedia of Complexity and Systems Science*, Springer, (2022), 203–220.

[17] R.H. Holdahl and K. Lie, Unconditionally stable splitting methods for the shallow water equations, *BIT*, **39** (1999), 451–472.

[18] H. Holden and X. Raynaud, Convergence of a finite difference scheme for the Camassa-Holm equation, *SIAM J. Numer. Anal.*, **44** (2006), 1655–1680.

[19] D.D. Holm and J.E. Marsden, Momentum maps and measure-valued solutions (peakons, filaments, and sheets) for the EPDiff equation, in: *The Breadth of Symplectic and Poisson Geometry, Progress in Mathematics*, Vol. 232, Birkhäuser, (2005), 203–235.

[20] D.D. Holm, J.E. Marsden, and T.S. Ratiu, Euler-Poincaré equations and semi-direct products with applications to continuum theories, *Adv. Math.*, **137** (1998), 1–81.

[21] D.D. Holm, L. Náraigh, and C. Tronci, Singular solutions of a modified two-component Camassa-Holm equation, *Phys. Rev. E*, **79** (2009), 016601.

[22] C. Jiang, Y. Gong, W. Cai, and Y. Wang, A linearly implicit structure-preserving scheme for the Camassa-Holm equation based on multiple scalar auxiliary variables approach, *J. Sci. Comput.*, **83**:20 (2020), 1–20.
[23] D. Ketcheson, Relaxation Runge-Kutta methods: Conservation and stability for inner-product norms, *SIAM J. Numer. Anal.*, **57**:6 (2019), 2850–2870.
[24] I. Kinnmark, *The Shallow Water Wave Equations: Formulation, Analysis and Application*, Springer, 1986.
[25] D. Li and X. Li, Multiple relaxation exponential Runge-Kutta methods for the nonlinear Schrödinger equation, *SIAM J. Numer. Anal.*, **62**:6 (2024), 2719–2744.
[26] D. Li, X. Li, J. Zhang, and Z. Zhang, Stabilized multiple-relaxation implicit-explicit Runge-Kutta methods for nonlinear Gross-Pitaevskii equations, *J. Comput. Phys.*, **538** (2025), 114183.
[27] D. Li, X. Li, and Z. Zhang, Linearly implicit and high-order energy-preserving relaxation schemes for highly oscillatory Hamiltonian systems, *J. Comput. Phys.*, **477** (2023), 1–19.
[28] X. Li, J. Wen, and D. Li, Mass- and energy-conserving difference schemes for nonlinear fractional Schrödinger equations, *Appl. Math. Lett.*, **111** (2021), 1–7.
[29] H.L. Liu and P. Terrance, On invariant-preserving finite difference schemes for the Camassa-Holm equation and the two-component Camassa-Holm system, *Commun. Comput. Phys.*, **19** (2016), 1015–1041.
[30] H. Liu and Y. Xing, An invariant preserving discontinuous Galerkin method for the Camassa-Holm equation, *SIAM J. Sci. Comput.*, **38** (2016), 1919–1934.
[31] J. Lu, Y. Xu, and C. Zhang, Error estimates of the local discontinuous Galerkin methods for two-dimensional (μ)-Camassa-Holm equations, *J. Comput. Appl. Math.*, **420** (2023), 114722.
[32] T. Matsuo, A Hamiltonian-conserving Galerkin scheme for the Camassa-Holm equation, *J. Comput. Appl. Math.*, **234** (2010), 1258–1266.
[33] T. Matsuo and H. Yamaguchi, An energy-conserving Galerkin scheme for a class of nonlinear dispersive equations, *J. Comput. Phys.*, **228** (2009), 4346–4358.
[34] Y. Miyatake, T. Matsuo, and D. Furihata, Conservative finite difference schemes for the modified Camassa-Holm equation, *JSIAM Lett.*, **3** (2011), 37–40.
[35] J. Pedlosky, *Geophysical Fluid Dynamics*, Springer, 1987.
[36] S.P. Popov, Numerical study of peakons and k-solitons of the Camassa-Holm and Holm-Hone equations, *Comput. Math. Math. Phys.*, **51** (2011), 1231–1238.
[37] D.T. Resio, Shallow-water waves, *J. Waterw. Port Coast. Ocean Eng.*, **113**:3 (1987), 264–281.
[38] G.M. Reznik, V. Zeitlin, and M.B. Jelloul, Nonlinear theory of geostrophic adjustment. Part 1. Rotating shallow-water model, *J. Fluid Mech.*, **445** (2001), 93-120.
[39] W.T. Tan, *Shallow Water Hydrodynamics: Mathematical Theory and Numerical Solution for a Two-Dimensional System of Shallow-Water Equations*, Elsevier, 1992.
[40] N. Tao, A decoupled and conservative difference scheme with fourth-order accuracy for the symmetric regularized long wave equations, *Appl. Math. Comput.*, **219** (2013), 9461–9648.
[41] X. Wang, An energy-preserving finite difference scheme with fourth-order accuracy for the generalized Camassa-Holm equation, *Commun. Nonlinear Sci. Numer. Simul.*, **119** (2023), 107121.
[42] Z.Q. Wang and X.M. Xiang, Generalized Laguerre approximations and spectral method for the Camassa-Holm equation, *IMA J. Numer. Anal.*, **35**:3 (2015), 1456–1482.
[43] Y. Xu and C. Shu, A local discontinuous Galerkin method for the Camassa-Holm equation, *SIAM J. Numer. Anal.*, **46**:4 (2008), 1998–2021.
[44] K. Yan and Y. Liu, The initial-value problem to the modified two-component Euler-Poincaré equations, *SIAM J. Numer. Anal.*, **54**:2 (2022), 2006–2039.
[45] T. Yan, J. Zhang, and Q. Zhang, Fully conservative difference schemes for the rotation-two-component Camassa-Holm system with smooth/nonsmooth initial data, *Wave Motion*, **129** (2024), 103333.
[46] X. Yang, Linear, first and second-order, unconditionally energy stable numerical schemes for the

phase field model of homopolymer blends, *J. Comput. Phys.*, **327** (2016), 294–316.

[47] X. Yang, J. Zhao, and X. He, Linear, second order and unconditionally energy stable schemes for the viscous Cahn-Hilliard equation with hyperbolic relaxation using the invariant energy quadratization method, *J. Comput. Appl. Math.*, **343** (2018), 80–97.

[48] V. Zeitlin, *Geophysical Fluid Dynamics: Understanding (Almost) Everything with Rotating Shallow Water Models*, Oxford University Press, 2018.

[49] Q. Zhang, L. Liu, and Z. Zhang, Linearly implicit invariant-preserving decoupled difference scheme for the rotation-two-component Camassa-Holm system, *SIAM J. Sci. Comput.*, **44** (2022), 2226–2252.

[50] Q. Zhang, T. Yan, and G. Gao, The energy method for high-order invariants in shallow water wave equations, *Appl. Math. Lett.*, **142** (2023), 108626.

[51] Q. Zhang, T. Yan, D. Xu, and Y. Chen, Direct/split invariant-preserving Fourier pseudo-spectral methods for the rotation-two-component Camassa-Holm system with peakon solitons, *Comput. Phys. Commun.*, **302** (2024), 109237.

[52] Q. Zhang, J.Y. Zhang, and Z.M. Zhang, Error estimates of invariant-preserving difference schemes for the rotation-two-component Camassa-Holm system with small energy, *Calcolo*, **61** (2024), 9.

[53] Y. Zhang and Y. Cao, A fuzzy quantification approach of uncertainties in an extreme wave height modeling, *Acta Oceanolog. Sin.*, **34**:3 (2015), 90–98.

[54] Z. Zhang, C. Luo, and Z. Zhao, Application of probabilistic method in maximum tsunami height prediction considering stochastic seabed topography, *Nat. Hazard.*, **104**:3 (2020), 2511–2530.